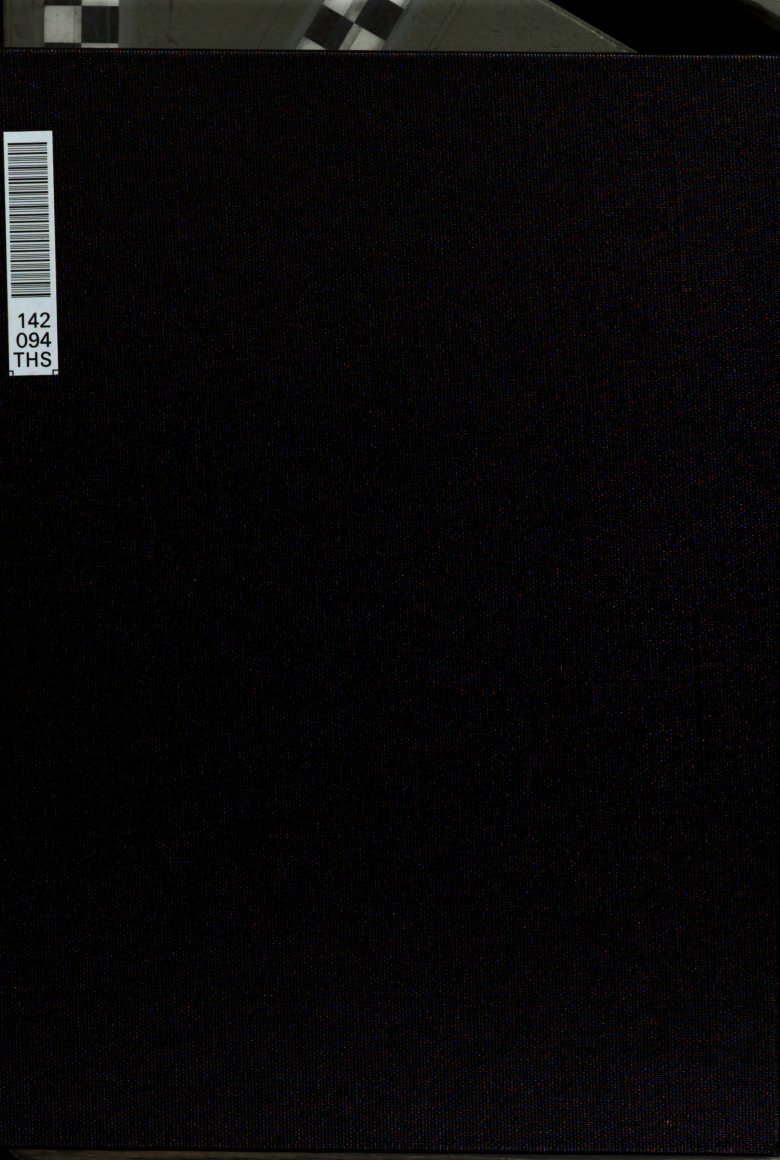

This is to certify that the
dissertation entitled

MATHEMATICAL MODELING AND COMPUTATION OF THE OPTICAL RESPONSE FROM NANOSTRUCTURES

presented by

Yuanchang Sun

has been accepted towards fulfillment
of the requirements for the

Doctoral degree in Mathematics

Major Professor's Signature

06/24/2009

Date

MATHEMATICAL MODELING AND COMPUTATION OF THE OPTICAL RESPONSE FROM NANOSTRUCTURES

By

Yuanchang Sun

A DISSERTATION

Submitted to
Michigan State University
in partial fulfillment of the requirements
for the degree of

DOCTOR OF PHILOSOPHY

Mathematics

2009

ABSTRACT

MATHEMATICAL MODELING AND COMPUTATION OF THE OPTICAL RESPONSE FROM NANOSTRUCTURES

By

Yuanchang Sun

This dissertation studies the computational modeling for nanostructures in response to external electromagnetic fields. Light-matter interactions on nanoscale are at the heart of nano-optics. To fully characterize the optical interactions with nanostructures quantum electrodynamics (QED) must be invoked, however, the required extremely intense computation and analysis prohibit QED from applications in nano-optics. To avoid the expensive computations and be able to seize the essential quantum effects a semiclassical model is developed. The wellposedness of the model partial differential equations is established. Emphasis is placed on the optical interactions with an individual nanostructure, excitons and biexcitons effects and finite-size effects are investigated.

The crucial step of our model is to couple the electromagnetic fields with the motion of the excited particles to yield a new dielectric constant which contains quantum effects of interest. A novel feature of the dielectric constant is the wavevector-dependence which leads to a multi-wave propagation inside the medium. Additional boundary conditions are proposed to deal with this situation. We proceed with incorporating this dielectric constant to Maxwell's equations, and by solving a scattering problem the quantum effects can be captured in the scattered spectra.

To my parents

ACKNOWLEDGMENTS

I would like to give my deepest and sincerest gratitude to my advisor, Professor Gang Bao, for his constant encouragement and support during my graduate study at Michigan State University. His knowledge, insights and enthusiasm are invaluable.

I would also express my thanks to Professor Andrew Christlieb, Professor Di Liu, Professor Jianliang Qian and Professor Zhengfang Zhou for their time, efforts and valuable suggestions. Professor Peijun Li deserves my special thanks for his continuous help and useful discussions.

I am very grateful to my classmates Zhengfu, KiHyun, Junshan, Yuliang and Tianshuang for the wonderful time together. Last, but not least, I want to thank Ling, my wife, for her support during these years.

TABLE OF CONTENTS

LIST OF FIGURES

Chapter 1

INTRODUCTION

The study of the propagation of light waves in nanostructured media has generated numerous interests among scientific and industrial communities over the past decade. Because of the tiny structural scales, some quantum effects which are negligible macroscopically dominate among factors in shaping the optical properties of such structures. Modeling and computations of nano optical response hence become an increasing demand in technical applications and designs of nanostructures, exploitations of quantum effects are another obvious driving force behind.

Consider an optically excited semiconductor, excitons are formed in response to the applied field. An exciton is a quantum of electronic excitation energy traveling in a semiconductor, lots of research works have been devoted to the study of the exciton effects since the concept of exciton was first introduced by Frenkel in 1931 [21]. The fundamental importance of the excitons is clear; they play an essential role in optical effects such as luminescence, fluorescence, photographic process, photoconductivity,

and so on [36]. These various features enable semiconductors to be widely used in numerous fields, including optical communication, computing, biomedical imaging, and data storage. The optical properties of excitons in bulk semiconductors have been extensively studied (see Chap. 13 of [33] and references therein). For the excitons in structures of reduced dimensionality, for example, in nanostructured semiconductors like quantum well, quantum wire and quantum dot, the states of the exciton shifts to higher energy as the size of structure decreases. This situation is called quantum confinement effect, which makes nanoscale semiconductor cease to resemble bulk, exhibits strikingly different properties instead [50, 66]. Furthermore, the interactions between excitons should be taken into account if large density of excitons is produced in a material. Provided the interaction is attractive, two excitons could bind to form a biexciton. The exciton to biexciton transition confined in nanostructures has been observed and studied by many groups, and some resonance phenomena, e.g., electromagnetic induced transparency, were reported in [7, 11]. While some physicists have begun to address a few of the challenging problems in these areas[12, 32, 57, 58], the mathematical formulation and efficient numerical algorithms remain open. The dissertation work is an initial attempt of the mathematical modeling and numerical computations of the quantum confinement effects of excitons.

It should be emphasized that the understanding of excitons was made possible only after the discovery of quantum theory. Based on this understanding, the quantum mechanics are invoked to characterize the excitation of the nanostructure (viewed

as an ensemble of charged particles), and microscopic Maxwell's equations are employed to govern the wave propagation. The two equations are bridged via the dipole moment operator which is a key factor for the derivation of a new dielectric constant. The resulting equations are a coupled system which is difficult to derive and solve mainly for two reasons; Firstly, the wavefunctions and eigenenergies on atomic scales are usually assumed to be known, whereas the many-body Schrödinger equations are not completely solvable. Approximations have to be made for systems containing large numbers of particles. Secondly, a set of integro-differential equations must be solved and usually analytical solution are not achievable. Often numerical schemes need to be developed to attain solutions. Instead of solving a many-body problem, we approximate the wavefunctions via a perturbation argument. The induced polarization in the quantum picture then can be calculated, and it will serve as a source term to Maxwell's equations. By choosing suitable numerical methods, the solution of Maxwell's equations provides an insight to investigate the exciton effects on nanoscales.

This work is structured as follows. Chapter 2 provides a brief review of the most important concepts of electromagnetics and quantum mechanics, the central problems in nano-optics are also introduced. Subsequently, the design and mathematical analysis of a semiclassical model are presented in Chap. 3 and Chap. 4, respectively. In particular, Chap. 3 is devoted to a description of modeling approaches both in classical and quantum pictures, special emphasis is the derivation of wavevector-

dependent dielectric constant. In addition, the effects of finite-size are discussed as an open issue. Chap. 4 deals with the mathematical issues in the model partial differential equations. Boundary value problems are derived along with additional boundary conditions. Existence and uniqueness results are obtained. The numerical experiments in Chap. 5 are specially designed to show the validity of our model. In Chap. 6 a summary of the thesis is presented and future directions are discussed.

Chapter 2

BACKGROUND

To describe the optical radiation on nanoscale the field theory based on Maxwell's equations is required. To characterize the optical properties of the nanostructures with which the light fields interact a quantum description is necessary. This section summarizes the fundamentals of these principles forming a basis for the following chapters. For more thorough treatments the reader is referred to [8, 29] on electromagnetism and [22, 54] on quantum mechanics. This chapter starts with Maxwell's equations established by James Clerk Maxwell in 1870s.

2.1 Electrodynamics in matter

The spatial and temporal evolution of electromagnetic fields is described by electrodynamics which was founded in 19th century by Maxwell. The theory can correctly predict the propagation of electric and magnetics fields and their interactions in the presence of charges, currents and any type of matter, and it constitutes a set of four

elegant equations known as Maxwell's equations. In the Gaussian unit, the equations have the form

$$\begin{cases} \nabla \cdot \mathbf{D}(\mathbf{r},t) = 4\pi\rho(\mathbf{r},t) \,, \\ \nabla \times \mathbf{E}(\mathbf{r},t) = -\frac{1}{c}\frac{\partial \mathbf{B}(\mathbf{r},t)}{\partial t} \,, \\ \nabla \cdot \mathbf{B}(\mathbf{r},t) = 0 \,, \\ \nabla \times \mathbf{H}(\mathbf{r},t) = \frac{1}{c}\frac{\partial \mathbf{D}(\mathbf{r},t)}{\partial t} + \frac{4\pi}{c}\mathbf{j}(\mathbf{r},t) \,, \end{cases} \tag{2.1.1}$$

where $\mathbf{E}$ denotes the electric field, $\mathbf{D}$ the electric displacement, $\mathbf{H}$ the magnetic field, $\mathbf{B}$ the magnetic induction, the constant c is known as the vacuum speed of light, $\mathbf{j}$ the current density, and ρ the charge density. The electromagnetic properties of the medium are most commonly discussed in terms of the polarization $\mathbf{P}$ and magnetization $\mathbf{M}$ according to

$$\mathbf{D}(\mathbf{r},t) = \mathbf{E}(\mathbf{r},t) + 4\pi\mathbf{P}(\mathbf{r},t) \,, \mathbf{H}(\mathbf{r},t) = \mathbf{B}(\mathbf{r},t) - 4\pi\mathbf{M}(\mathbf{r},t) \,.$$

Therefore, in vacuum $\mathbf{E} \equiv \mathbf{D}$, $\mathbf{B} = \mathbf{H}$. In addition, the charge conservation is implicitly contained in Maxwell's equations. Taking the divergence of the last equation in Eq. 2.1.1, noting that $\nabla \cdot \nabla \times \mathbf{H}$ is identical zero, and substituting the first equation for $\nabla \cdot \mathbf{D}$ one obtains the continuity equation

$$\nabla \cdot \mathbf{J}(\mathbf{r},t) + \frac{\partial \rho(\mathbf{r},t)}{\partial t} = 0 \,.$$

After substituting the fields $\mathbf{D}$ and $\mathbf{B}$ in the Maxwell's *curl* equations and combining the two resulting equations we obtain the following wave equations

$$\nabla \times \nabla \times \mathbf{E} + \frac{1}{c^2}\frac{\partial^2 \mathbf{E}}{\partial t^2} = -\frac{4\pi}{c^2}\frac{\partial}{\partial t}\left(\mathbf{j} + \frac{\partial \mathbf{P}}{\partial t} + c\nabla \times \mathbf{M}\right), \tag{2.1.2}$$

$$\nabla \times \nabla \times \mathbf{H} + \frac{1}{c^2}\frac{\partial^2 \mathbf{H}}{\partial t^2} = \frac{4\pi}{c}\left(\nabla \times \frac{\partial \mathbf{P}}{\partial t} + \nabla \times \mathbf{j} + \frac{\partial^2 \mathbf{M}}{\partial t^2}\right). \tag{2.1.3}$$

The expression in the bracket of Eq. (2.1.2) can be associated to the *total current density* $\mathbf{j}_t = \mathbf{j}_s + \mathbf{j}_c + \frac{\partial \mathbf{P}}{\partial t} + c\nabla \times \mathbf{M}$, where $\mathbf{j}$ is split into a *source current density* $\mathbf{j}_s$ and an induced *conduction current density* $\mathbf{j}_c$. The terms $\frac{\partial \mathbf{P}}{\partial t}$ and $\nabla \times \mathbf{M}$ are recognized as the *polarization current density* $\mathbf{j}_p$ and the *magnetization current density* $\mathbf{j}_m$. In most practical applications, such as scattering problems, there are no source currents or charges present. However, to study the fields inside a medium the induced polarization by the excited charges serves as a source term in the equations.

Since the material properties are discontinuous on the boundaries, knowledge of the variation of fields quantity across an interface is often necessary in solving or formulating electromagnetic problems. These boundary conditions can be given as [8]

$$\mathbf{n} \times (\mathbf{E}_1 - \mathbf{E}_2) = \mathbf{0} \text{ on } \Gamma,$$

$$\mathbf{n} \times (\mathbf{H}_1 - \mathbf{H}_2) = \mathbf{K} \text{ on } \Gamma,$$

$$\mathbf{n} \cdot (\mathbf{D}_1 - \mathbf{D}_2) = \sigma \text{ on } \Gamma,$$

$$\mathbf{n} \cdot (\mathbf{B}_1 - \mathbf{B}_2) = 0 \text{ on } \Gamma ,$$

where $\mathbf{n}$ is the unit normal vector on the boundary Γ. $\mathbf{K}$ and σ are the surface current and charges on the boundary, respectively.

Often the fields of interest vary harmonically (sinusoidally) with time. The time dependence in the wave equations can be easily separated to obtain a harmonic differential equation. Here, a monochromatic field can be written as

$$\mathbf{E}(\mathbf{r}, t) = \mathrm{Re}\{\mathbf{E}(\mathbf{r}) \exp(-i\omega t)\} .$$

With similar expressions for the other fields. Notice that $\mathbf{E}(\mathbf{r}, t)$ is real, whereas the spatial part $\mathbf{E}(\mathbf{r})$ is complex. The symbol $\mathbf{E}$ will be used for both, the real, time-dependent field and the complex spatial part of the field. The Maxwell equations can then be written as

$$\begin{cases} \nabla \cdot \mathbf{D}(\mathbf{r}) = 4\pi\rho(\mathbf{r}) , \\ \nabla \times \mathbf{E}(\mathbf{r}) = +\frac{i\omega}{c}\mathbf{B}(\mathbf{r}) , \\ \nabla \cdot \mathbf{B}(\mathbf{r}) = 0 , \\ \nabla \times \mathbf{H}(\mathbf{r}) = -\frac{i\omega}{c}\mathbf{D}(\mathbf{r}) + \frac{4\pi}{c}\mathbf{j}(\mathbf{r}) , \end{cases} \tag{2.1.4}$$

2.1.1 Microscopic Maxwell's equations

This set of equations together with the appropriate boundary conditions can successfully determine the time and spatial evolution of electromagnetic fields in the presence of a matter. Both the above equations and Eq. (2.1.1) belong to macroscopic elec-

tromagnetic theory of bulk media, all the variables are averaged quantities. However, when the size of medium reduces to nanoscale, although small compared to the wavelength, the medium consists of many charged particles. On a macroscopic scale the charged density ρ and current density $\mathbf{j}$ can be treated as continuous functions. But the discrete charges are spatially separated. Thus, the microscopic structure of matter is not considered in macroscopic Maxwell's equations. In order to derive the optical responses of a nanoscale system it is essential to consider the fields which are created by atomic electric charges in motion. In this case, we must carry out a microscopic treatment of the electromagnetic fields and set

$$\rho(r) = \sum_l e_l \delta(\mathbf{r} - \mathbf{r}_l) \ , \mathbf{j}(r) = \sum_l e_l \mathbf{v}_l \delta(\mathbf{r} - \mathbf{r}_l) \ ,$$

where $\mathbf{v}_l$ is the velocity of the $l-$th charged particle.

Hence the so called **Microscopic Maxwell's equations** take the following form

$$\begin{cases} \nabla \cdot \mathbf{E} = 4\pi\rho \\ \nabla \times \mathbf{E} = -\frac{1}{c}\frac{\partial \mathbf{H}}{\partial t} \\ \nabla \cdot \mathbf{H} = 0 \\ \nabla \times \mathbf{H} = \frac{1}{c}\frac{\partial \mathbf{E}}{\partial t} + \frac{4\pi}{c}\mathbf{j} \end{cases} \tag{2.1.5}$$

This set of equations are the most basic ones, which describe the electric field $\mathbf{E}$ and the magnetic field $\mathbf{H}$ in vacuum, together with their sources (charge- and current-densities). That is, it is assumed that there is no other ponderable matter in the

system than the charges and currents accounted for in the equations. There several ways of deducing the macroscopic equations from their microscopic counterparts (see [63] for example). To derive the polarization of the charge distribution we consider the total current density

$$\mathbf{j} = \frac{\partial \mathbf{P}}{\partial t}. \tag{2.1.6}$$

we ignored the contribution of the source current $\mathbf{j}_s$ which generates the incident field since it is not part of the considered particle. Furthermore, we incorporate the conduction current $\mathbf{j}_c$ into the polarization current. The optical response is given by the polarization $\mathbf{P}$ induced on the matter is

$$\mathbf{P} = \langle \Psi | \hat{\mu} | \Psi \rangle = \int \Psi^* \hat{\mu} \Psi \mathrm{d}r \ ,$$

where $\hat{\mu}$ is the polarization operator. $\langle \Psi | \hat{\mu} | \Psi \rangle$ stands for the expectation value of operator $\hat{\mu}$ in Dirac's notation. Ψ is the wavefunction of the matter under the applied field. Next part will be dedicated to the Schrödinger equation with Ψ being its solution.

2.2 Quantum mechanics in nano-optics

Nanostructures or nano optical materials can capture and manipulate light in many amazing ways, and they may possess drastically different optical properties from their bulk counterparts. To get insights of the optical responses of these structures, an ac-

curate characterization of excitations in them for an applied field becomes essentially important. As we move to smaller and smaller scales the underlying physical laws change from macroscopic to microscopic, some quantum effects start to dominate in shaping the material properties. The quantum mechanics hence must be invoked to fully characterize the evolution of the matter states on nanometer scales. The following section is devoted to some fundamentals and basic concepts in quantum mechanics. In particular the Schrödinger equations will be briefly discussed.

2.2.1 Schrödinger equations

Quantum mechanics is a set of principles underlying the most fundamental known description of all physical systems at the submicroscopic scale. It is essential to understand the behavior of systems at atomic scales and smaller. In the development of quantum mechanics, Planck's quantum theory, Bohr's postulates, and de Broglie's hypothesis represented very important steps. However, they are overshadowed by the discovery of a fundamental differential equation describing the electron and accounting for its wave properties, and the construction of a theory accounting for the quantum nature of radiation. The crucial move in this connection was made by Schrödinger in 1926 when he proposed a partial differential equation that turns out to be generally applicable to the motion of charged particles in the nonrelativistic regime ($v \ll c$). Schrödinger equation is as central to quantum mechanics as Newton's laws are to classical mechanics.

The time dependent Schrödinger equation for a general quantum system is of the form

$$i\hbar\frac{\partial}{\partial t}\Psi(\mathbf{r},t) = \hat{H}\Psi(\mathbf{r},t)\ , \tag{2.2.1}$$

where i is the imaginary unit, $\hbar$ is the Reduced Planck's constant (Planck's constant divided by 2π), the wavefunction $\Psi(\mathbf{r},t)$ which describes the behavior of the system may be statistically interpreted by means of the Schrödinger theory. In particular, the quantity $\Psi^*(\mathbf{r},t)\Psi(\mathbf{r},t) = |\Psi|^2$, which plays the role of a distribution function, represents the *probability density*, or probability of the system in any of possible states; $\hat{H}$ stands for the Hamiltonian operator which is a Hermitian operator. Take a single particle in three dimensions as an example, the Schrödinger equation takes the form

$$i\hbar\frac{\partial}{\partial t}\Psi(\mathbf{r},t) = -\frac{\hbar^2}{2M}\nabla^2\Psi(\mathbf{r},t) + V(\mathbf{r})\Psi(\mathbf{r},t)\ ,$$

where $\mathbf{r} = (x,y,z)$ is the particle's position in three-dimensional space; $\Psi(\mathbf{r},t)$ is the wavefunction, which is the amplitude for the particle to have a given position $\mathbf{r}$ at any given time t; M is the mass of the particle. Here the Hamiltonian operator reads $\hat{H} = -\frac{\hbar^2}{2M}\nabla^2 + V(\mathbf{r})$, $V(\mathbf{r})$ is the time independent potential energy of the particle at each position $\mathbf{r}$ and ∇^2 is the Laplace operator.

Consider the optical interactions of a nanoscale medium and light which are encountered in various fields of research. For instance: the activity of proteins and other macromolecules is followed by optical techniques; optically excited single mole-

cules are used to probe their local environment; and optical interactions with metal nanostructures are actively investigated because of their resonant behavior important for sensing applications. Furthermore, various nanoscale structures are encountered in near-field optics as local light sources. All above matters or structures are small compared to the wavelength of light, and they consists of many charged particles. To describe the behavior of this many-particle (N particles) system in response to an electromagnetic radiation $\mathbf{E}(\mathbf{r}, t)$ (laser beam for example), the general Hamiltonian takes the form

$$\hat{H}_M = H_0 + H_{\text{int}} ,$$

which is written as the sum of the Hamiltonian H_0 for the matter system and an interaction Hamiltonian, H_{int}, which describes the interaction of the matter with the electromagnetic field. Usually, we take them to be the following forms [10]

$$H_0 = \sum_{l,j} \left\{ \frac{1}{2m_l} \mathbf{p}_l^2 + V(\mathbf{r}_l, \mathbf{r}_j) \right\} , \tag{2.2.2}$$

$$H_{int} = -\sum_{l} e_l \mathbf{r}_l \cdot \mathbf{E}(\mathbf{r}_l, t) , \tag{2.2.3}$$

where e_l, m_l, $\mathbf{r}_l$ and $\mathbf{p}_l$ are the charge, mass, coordinate and conjugate momentum of the coordinate, respectively, for the lth particle, $V(\mathbf{r}_l, \mathbf{r}_j)$ is the potential interaction energy of the lth and jth particles. We assume that $\mathbf{E}(\mathbf{r}, t)$ can be represented as a

discrete sum of (positive and negative) frequency component as

$$\mathbf{E}(\mathbf{r},t) = \sum_{\omega} \tilde{\mathbf{E}}(\mathbf{r},\omega)\exp(-i\omega t)\ .$$

So (3.2.1) can also be written as $-\sum_{\omega}\int d\mathbf{r}\hat{\mathbf{P}}(\mathbf{r})\cdot\tilde{\mathbf{E}}(\mathbf{r},t)\exp(-i\omega t)$, where $\hat{\mathbf{P}}(\mathbf{r}) = \sum_l e_l\mathbf{r}\delta(\mathbf{r}-\mathbf{r}_l)$ is the electric dipole moment operator.

The wavefunction $\Psi(\mathbf{r},t) = \Psi(\mathbf{r}_1,\cdots,\mathbf{r}_N,t)$ satisfies

$$i\hbar\frac{\partial}{\partial t}\Psi(\mathbf{r},t) = \hat{H}_M\Psi(\mathbf{r},t)\ . \tag{2.2.4}$$

In general, V has contributions from all four fundamental interactions so far known, namely strong, electromagnetic, weak, and gravitational interactions. For the behavior of electrons only the electromagnetic contribution is of importance, and within the electromagnetic interaction the electrostatic potential is dominant. Since the masses of nuclei are much greater than the mass of an electron, the nuclei move much slower than the electron. This allows the electrons to practically instantaneously follow the nuclear motion. For an electron, the nucleus appears to be at rest. This is the essence of Born-Oppenheimer approximation which allows us to separate the nuclear wavefunction from the electronic one. We can restrict the index l in Eq. (2.2.2) to run only over electron coordinates. In the case of $\hat{H}_M = H_0$ we can separate the t and $\mathbf{r}$ dependence as

$$\Psi(\mathbf{r},t) = \sum_{n=1}^{\infty} \mathrm{e}^{-i/\hbar E_n t}\varphi_n(\mathbf{r})\ ,$$

where φ_n and E_n are the eigenfunction and eigenvalues of $\hat{H}_0$, i.e., $\hat{H}_0\varphi_n(\mathbf{r}) = E_n\varphi_n(\mathbf{r})$.

After the radiation field is turned on, the system experiences an external, time-dependent perturbation represented by the interaction Hamiltonian H_{int}. A perturbation method will be discussed to obtain the wavefunction in the next chapter.

2.2.2 Dirac's notation and operators

In quantum mechanics it is very common to write the Schrödinger equation (2.2.1) using the so called Dirac's notation.

$$i\hbar\frac{\partial}{\partial t}|\psi(t)\rangle = \hat{H}|\psi\rangle \ . \tag{2.2.5}$$

In the following section I will briefly introduce the Dirac's notation which has many advantages, especially from the physicist's point of view. In addition the basic mathematics of vector space as used in quantum mechanics will be formulated. The reader is referred to [54] for a detailed discussion.

Ket Space. Consider a complex vector space whose dimensionality is specialized to physical system. In quantum mechanics a physical state, for example, an atom with definite spin orientation, is represented by a **state vector** in a complex vector space. Following Dirac, we call such a vector a **ket** and denote it by $|\alpha\rangle$. This state ket is postulated to contain complete information about the physical state. Two kets can be added: $|\alpha\rangle + |\beta\rangle = |\gamma\rangle$. The sum $|\gamma\rangle$ is another ket. If $|\alpha\rangle$ is multiplied by

a complex number c, the resulting product $c|\alpha\rangle$ is another ket. One remark is that $|\alpha\rangle$ and $c|\alpha\rangle$, with $c \neq 0$, represent the same physical state. In other words, only the "direction" in vector space is of significance.

An **observable**, such as momentum and energy, can be represented by an **operator**, such as A. Generally an operator acts in a ket from the left

$$A \cdot |\alpha\rangle = A|\alpha\rangle \ , \tag{2.2.6}$$

which is another ket.

In general, $A|\alpha\rangle$ is not a constant times $|\alpha\rangle$. However, there are particular kets of importance, known as **eigenkets** of operator A, denoted by $|a\rangle, |b\rangle$, with the property

$$A|a\rangle = a|a\rangle, A|b\rangle = b|b\rangle \ , \tag{2.2.7}$$

where a, b are just numbers. The physical state corresponding to an eigenket is called an **eigenstate**.

Bra Space and Inner Products. The vector space we have introduced is a ket space. The notation of a **bra space**, a vector space "dual to" the ket space will be discussed in the following. We postulate that corresponding to every ket $|\alpha\rangle$ there exists a bra, denoted by $\langle\alpha|$, in this dual, or bra, space. Roughly speaking, we can regard as some kind of mirror image of the ket space.

The bra dual to $c|\alpha\rangle$ is postulated to be $c^*\langle\alpha|$, not $c\langle\alpha|$, which is a very important

point. More generally, we have the bra dual of $c_\alpha|\alpha\rangle + c_\beta|\beta\rangle$ being $\overset{*}{c}_\alpha\langle\alpha| + c^*_\beta\langle\beta|$. We now define the **inner product** of a bra and a ket. The product is written as a bra standing on the left and a ket standing on the right, for example

$$\langle\beta|\alpha\rangle = (\langle\beta|) \cdot (|\alpha\rangle) \ .$$

This product is, in general, a complex number. Two fundamental property of the inner product are postulated as follows. First, $\langle\beta|\alpha\rangle = \langle\alpha|\beta\rangle^*$. Second, $\langle\alpha|\alpha\rangle \geq 0$, where the equality sign holds only if $|\alpha\rangle = 0$, or called null ket. Two kets $|\alpha\rangle$ and $|\beta\rangle$ are said to be orthogonal if $\langle\beta|\alpha\rangle = 0$.

Operators. As I mentioned earlier, observables like momentum and energy are to be represented by operators that can act on kets from the left

$$X \cdot (|\alpha\rangle) = X|\alpha\rangle \ ,$$

and the resulting product is another ket. Operators X and Y are said to be equal if $X|\alpha\rangle = Y|\alpha\rangle$ for any ket in the ket space. An operator X always acts on a bra from the right side $(\langle\alpha|) \cdot X = \langle\alpha|X$, and the resulting product is another bra. The ket $X|\alpha\rangle$ and the bra $\langle\alpha|X$ are, in general, not dual to each other. We define $\langle\alpha|X^\dagger$ to be the dual of $X|\alpha\rangle$. The operator $X^\dagger$ is called the Hermitian adjoint of X. An operator X is said to be Hermitian if $X = X^\dagger$. Operators can be added; addition operations are commutative and associative: $X + Y = Y + X$, $X + (Y + Z) =$

$(X + Y) + Z$. Operators can be multiplied and multiplication operations are, in general, noncommutative, that is $XY \neq YX$. Multiplication operations are, however, associative: $X(YZ) = (XY)Z = XYZ$.

We have considered the following products: $\langle\alpha|\beta\rangle$, $X|\alpha\rangle$, $\langle\alpha|X^\dagger$ and XY. Let us multiply $|\beta\rangle$ and $\langle\alpha|$, in that order. The resulting product

$$(|\beta\rangle) \cdot (\langle\alpha|) = |\beta\rangle\langle\alpha|$$

is known as the **outer product** of $|\beta\rangle$ and $\langle\alpha|$. In fact, $|\beta\rangle\langle\alpha|$ is to be regarded as an operator which will be emphasized in a moment. It is hence fundamentally different from the inner product $\langle\alpha|\beta\rangle$. It is clear that multiplication operations among operators are associative. Actually the associative property is postulated to hold to deal with multiplications among kets, bras, and operators. Dirac calls this important postulate the associative axiom of multiplication. To illustrate the axiom we consider an outer product acting on a ket:

$$(|\beta\rangle\langle\alpha|) \cdot |\gamma\rangle \ ,$$

which is the same as $|\beta\rangle \cdot (\langle\alpha|\gamma\rangle)$, where $\langle\alpha|\gamma\rangle$ is a complex number. So the outer product acting on a ket is just another ket; in other words, $|\beta\rangle\langle\alpha|$ can be regarded as an operator. It is easy to see that if $X = |\beta\rangle\langle\alpha|$, then $X^\dagger = |\alpha\rangle\langle\beta|$. In a second

important illustration of the associative axiom, we note that

$$(\langle\beta|) \cdot (X|\alpha\rangle) = (\langle\beta|X) \cdot (|\alpha\rangle) \; .$$

Since the two sides are equal, we might use the more compact notation $\langle\beta|X|\alpha\rangle$. With all these concepts and properties we define the **expectation value** of an operator A taken with respect to state $|\alpha\rangle$ as $\langle A\rangle = \langle\alpha|A|\alpha\rangle$.

Chapter 3

PHYSICAL MODELS

The study of optical interactions with nanoscale systems (nanostructures) is at the heart of nano-optics. Unlike their bulk counterparts, nanostructures may control and manipulate lights in ways beyond our imaginations. The novel optical properties have made them promising candidates in various applications. Hence the relevant optical modeling of nanostructures has become an increasing demand. This chapter is devoted to the modeling approaches for the optical responses of nanostructures. Generally, it is a challenging task to build a good model for nano optical responses for several reasons; First, it contains multiple scales for which careful analysis needs to be made especially on the interfaces; Secondly, some quantum effects (for example, quantum confinement) becomes more important as scales getting smaller. Hence a rigorous characterization is a must to take the quantum effects into account; Finally, the resulting equations are usually a coupled system which poses many issues in terms of analysis and computations.

To completely understand light-matter interactions quantum electrodynamics (QED) needs to be employed. Although QED provides accurate characterizations of optical interactions with atoms and molecules, nanostructures are usually too complex and thus the required extremely intense computation prohibits QED from applications in nano-optics. Reader is referred to [13, 14, 38] for a thorough introduction of QED. Two types of modeling approaches will be introduced in this chapter: classical model and semiclassical model. In the Lorentz model the motions of charged particles and electromagnetic field are both treated classically. Cho's nonlocal response theory is a semiclassical approach which requires a quantum mechanical characterization for the moving charges, while treats the field using classical Maxwell's equations. In addition, two other types of approached by Keller and Stahl will be briefly mentioned in the chapter. Starting from the nonlocal response theory, a different semiclassical model is developed. The crucial step is to derive a wavevector-dependent dielectric constant which contains quantum confinement information and nonlocal effects as well. The model problem can then be solved by combining the new dielectric constant with the Maxwell equations. Hence by solving Maxwells equations for the fields, these quantum effects can be captured.

3.1 Modeling approaches

Consider a nanoscale medium exposed in a laser beam as illustrated in Fig. 3.1. We are interested in how this medium responds to the applied field, or how the optical

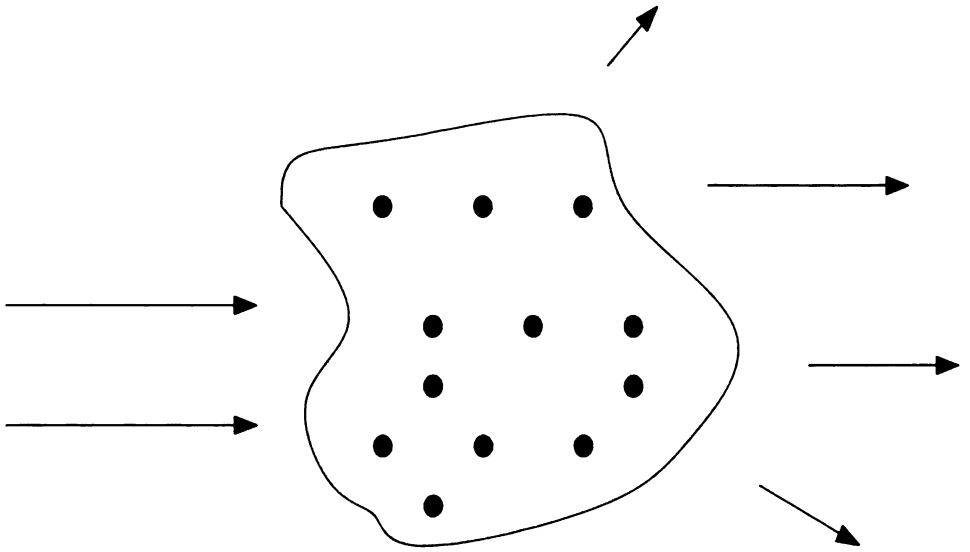

Figure 3.1: Optical interactions between a nanoscale medium and electromagnetic radiation.

properties are determined. Physically the external field will leads to the motion of a charged particle. The following Lorentz model offers the simplest picture of particle-field interactions. It is purely classical; however, this model is an elegant tool for visualizing particle–field interactions. The Lorentz Oscillator model also bears a number of basic insights into this problem. For a basic discussion of this model see [33, 40].

3.1.1 Lorentz model

Lorentz was a late nineteenth century physicist, and quantum mechanics had not yet been discovered. However, he did understand the results of classical mechanics and electromagnetic theory. Therefore, it is not surprising that he described the problem of atom-field interactions in these terms. Lorentz thought of an atom as a mass (the nucleus) connected to another smaller mass (the electron) by a spring, Fig. 3.2.

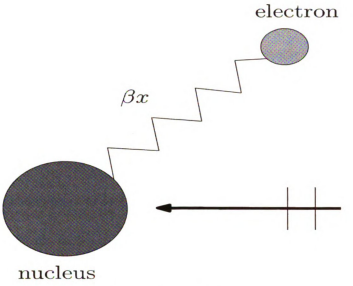

Figure 3.2: Lorentz Oscillator Model.

The spring would be set into motion by an electric field interacting with the charge of the electron. The field would either repel or attract the electron which would result in either compressing or stretching the spring. Lorentz was not positing the existence of a physical spring connecting the electron to an atom; however, he did postulate that the force binding the two could be described by Hooke's Law, i.e., $F(x) = -\beta x$, where x is the displacement from equilibrium.

If Lorentz's system comes into contact with an electric field, then the electron will simply be displaced from equilibrium. The oscillating electric field of the electromagnetic wave will set the electron into harmonic motion. The effect of the magnetic field can be omitted because it is miniscule compared to the electric field. Lorentz also considered the possibility of damping in his model.

The result of Lorentz's work was the Abraham–Lorentz Equation:

$$m\frac{\mathrm{d}^2}{\mathrm{d}x^2}x(t) + m\gamma\frac{\mathrm{d}}{\mathrm{d}x}x(t) + \beta x(t) = eE_0\mathrm{e}^{-i\omega t} \,. \tag{3.1.1}$$

This equation has one of the most well-known forms of mathematical physics. Here we assume that the mass m of every oscillator (electron) carries a charge e; $\beta = m\omega_0^2$ is the spring constant with ω_0 being the eigenfrequency. Lorentz understood the origin of all the terms in the equation except for the damping term. He really could not quantify γ. But this result is not surprising because the full interpretation of γ requires at least a semiclassical treatment of this problem. The main sources are atomic collisions, the Doppler effect, and spontaneous emission. The general solution of Eq. (3.1.1) is a sum of the general solution of the corresponding homogeneous equation and of a special solution of the inhomogeneous one. Correspondingly we assume the following ansatz:

$$x(t) = x_0 \exp\left[-i(\omega_0^2 - \gamma^2/4)^{1/2}t\right] \exp(-t\gamma/2) + x_p\mathrm{e}^{-i\omega t} \,. \tag{3.1.2}$$

The first term on the right hand side is the solution of the homogeneous equation and describes a transient feature. For $\omega_0^2 - \gamma^2/4 > 0$, one finds a damped oscillation with a damping-dependent eigenfrequency $(\omega_0^2 - \gamma^2/4)^{1/2}$. The above inequality defines the regime of weak damping. For stronger damping one gets essentially decaying term.

This transient feature disappears in any case after $t > \gamma^{-1}$. It is thus of importance for (ultra-) fast, time-resolved spectroscopy case. For the stationary, linear optics regime, we may safely omit this term. What is then left is a forced oscillation with amplitude x_p. Inserting the ansatz (3.1.2) into (3.1.1) we find the usual resonance term

$$x_p = \frac{eE_0}{m}(\omega_0^2 - \omega^2 - i\omega\gamma)^{-1} . \tag{3.1.3}$$

This oscillation is connected with a dipole moment of $\mu = ex_p$ and a polarizability $a(\omega) = \mu E_0$. The cumulative effects of all individual dipole moments of all electrons (oscillators) result in a polarization per unit volume $P = N\mu$, where N is the number of electrons per unit volume. It is known that the electric displacement

$$D = \varepsilon_0 E + P = \varepsilon_0 \left[1 + \frac{Ne^2}{\varepsilon_0 m}(\omega_0^2 - \omega^2 - i\omega\gamma)^{-1}\right] E$$

and

$$\varepsilon(\omega) = 1 + \frac{Ne^2}{\varepsilon_0 m}(\omega_0^2 - \omega^2 - i\omega\gamma)^{-1} .$$

Materials contain not only one type of oscillators and one resonance frequency ω_0, but many of them - like phonons, excitons etc. In linear optics, i.e. in linear response theory, we can just to sum over all response leading to

$$\varepsilon(\omega) = 1 + \sum_j \frac{Ne^2}{\varepsilon_0 m}(\omega_{0j}^2 - \omega^2 - i\omega\gamma)^{-1} .$$

3.1.2 Nonlocal response theory

Based on understanding the microscopic and nonlocal character of the nano optical responses, Cho and his group has developed a microscopic nonlocal response approach in [12]. The size- and shape-dependent response of nanoscale systems is due to the presence of size-quantized levels which should be described microscopically (quantum mechanically). Nonlocality appears as a straightforward consequence of quantum mechanical calculation of susceptibilities. The applied field $\mathbf{E}(\mathbf{r})$ at a point $\mathbf{r}$ induce polarization $\mathbf{P}(\mathbf{r})$, not only at the same position, but also at other positions within the extent of the relevant wavefunctions. Therefore, $\mathbf{P}$ is given as a function of $\mathbf{E}(\mathbf{r})$, namely

$$P(\mathbf{r}) = \int_{\mathrm{V}} \chi(\mathbf{r}, \mathbf{r}') \cdot \mathbf{E}(\mathbf{r}') \mathrm{d}\mathbf{r}' \, .$$

The framework of Cho's theory will be presented in the following, we start with rewriting Maxwell's equations (2.1.5) in frequency domain

$$\begin{cases} \nabla \cdot \mathbf{E}(\mathbf{r}) = 4\pi\rho(\mathbf{r}) \\ \nabla \times \mathbf{E}(\mathbf{r}) = \frac{i\omega}{c}\mathbf{H}(\mathbf{r}) \\ \nabla \cdot \mathbf{H}(\mathbf{r}) = 0 \\ \nabla \times \mathbf{H}(\mathbf{r}) = -\frac{i\omega}{c}\mathbf{E}(\mathbf{r}) + \frac{4\pi}{c}\mathbf{j}(\mathbf{r}) \, . \end{cases} \tag{3.1.4}$$

From now on ω will be dropped for simplicity purpose. Instead using the current density $\mathbf{j}$, sometimes it is more convenient to operate with polarization $\mathbf{P}$ since they

have the following relation (Fourier transformation of Eq. (2.1.6))

$$\mathbf{j}(\mathbf{r}) = -i\omega\mathbf{P}(\mathbf{r}) \,. \tag{3.1.5}$$

From Eq. (3.1.4)and (3.1.5), we eliminate the magnetic field $\mathbf{H}$ and obtain

$$\nabla \times \nabla \times \mathbf{E}(\mathbf{r}) - q^2\mathbf{E}(\mathbf{r}) = 4\pi k^2\mathbf{P}(\mathbf{r}) \tag{3.1.6}$$

with $q = \omega/c$ being the wavenumber in the free space.

For the nonlocal response as proposed in Cho's approach the polarization is related to $\mathbf{E}$ by

$$\mathbf{P}(\mathbf{r}) = \int \chi(\mathbf{r}, \mathbf{r}')\mathbf{E}(\mathbf{r}')\mathrm{d}r' \,, \tag{3.1.7}$$

From the first principle the susceptibility $\chi_{\xi\eta}$ in terms of polarization operator $\hat{P}$ is calculated as

$$\chi_{\xi\eta} = \sum_{\lambda}\left\{\frac{\langle 0|\hat{P}_\xi(\mathbf{r})|\lambda\rangle\langle\lambda|\hat{P}_\eta(\mathbf{r}')|0\rangle}{E_\lambda - \hbar\omega - i\delta^+} + \frac{\langle 0|\hat{P}_\eta(\mathbf{r}')|\lambda\rangle\langle\lambda|\hat{P}_\xi(\mathbf{r})|0\rangle}{E_\lambda + \hbar\omega + i\delta^+}\right\} . \tag{3.1.8}$$

The detailed derivation will be given in next part. Here E_λ and $|\lambda\rangle$ are the energy and eigenstate of the unperturbed hamiltonian H_0 and (ξ, η) are the components of Cartesian coordinates. The two terms of (3.1.8) are the resonant and nonresonant parts respectively. According to these two parts, the polarization $\mathbf{P}$ into resonant $\mathbf{P}_r$ and nonresonant $\mathbf{P}_{nr}$ parts. And the latter is assumed to be described by the

background susceptibility χ_b. The equation (3.1.6) can be changed to

$$\nabla \times \nabla \times \mathbf{E} - q^2\mathbf{E} = 4\pi q^2(\mathbf{P}_r + \mathbf{P}_{nr}) \,, \tag{3.1.9}$$

where $\mathbf{P}_{nr} = \chi_b\theta(\mathbf{r})\mathbf{E}(\mathbf{r})$, and $\theta(\mathbf{r}) = 1$ or 0 for $\mathbf{r}$ inside or outside the background medium, respectively. Then the above equation can be rewritten as

$$\nabla \times \nabla \times \mathbf{E} - q^2\varepsilon_{bg}\mathbf{E} = 4\pi q^2\mathbf{P}_r \tag{3.1.10}$$

with $\varepsilon_b = [1 + 4\pi\chi_b\theta(\mathbf{r})]$. The solution of (3.1.10) is given by

$$\mathbf{E}(\mathbf{r}) = \mathbf{E}_0(\mathbf{r}) + \int G(\mathbf{r},\mathbf{r}') \cdot \mathbf{P}_r(\mathbf{r}')\mathrm{d}r' \,, \tag{3.1.11}$$

Where $\mathbf{E}_0(\mathbf{r})$ is the solution of Eq.(3.1.10) for $\mathbf{P}(\mathbf{r}) = 0$, and the Green's function $G(\mathbf{r},\mathbf{r}')$ satisfies the equation

$$\nabla \times \nabla \times G(\mathbf{r},\mathbf{r}') - q^2\varepsilon_{bg}G(\mathbf{r},\mathbf{r}') = 4\pi\mathbf{I}\delta(\mathbf{r},\mathbf{r}') \tag{3.1.12}$$

with $\mathbf{I}$ being the identity operator.

Denote

$$\chi_{\xi\eta} = \sum_\lambda \frac{\langle 0|\hat{P}_\xi(\mathbf{r})|\lambda\rangle\langle\lambda|\hat{P}_\eta(\mathbf{r}')|0\rangle}{E_\lambda - h\omega - i\delta^+} = \sum_\lambda C_\lambda \rho_{\lambda\xi}(\mathbf{r})^* \rho_{\lambda\eta}(\mathbf{r}') \,, \tag{3.1.13}$$

where $C_\lambda(\omega) = 1/(E_\lambda - h\omega - i\delta^+)$ and $\rho_{\lambda\xi}(\mathbf{r}) = \langle 0|\hat{P}_\xi(\mathbf{r})|\lambda\rangle$.

Then we can write the polarization $\mathbf{P}_r(\mathbf{r})$ as the following

$$\begin{aligned}
\mathbf{P}_{\mathbf{r}\xi}(\mathbf{r}) &= \int \mathrm{d}r' \sum_{\eta=x,y,z} \chi_{\xi\eta}\mathbf{E}_\eta(\mathbf{r}') \\
&= \sum_\lambda C_\lambda(\omega) \int dr' \sum_{\eta=x,y,z} \rho_{\lambda\xi}(\mathbf{r})^* \rho_{\lambda\eta}(\mathbf{r}')\mathbf{E}_\eta(\mathbf{r}') \\
&= \sum_\lambda C_\lambda(\omega)\rho_{\lambda\xi}(\mathbf{r})^* \sum_{\eta=x,y,z} \int dr' \rho_{\lambda\eta}(\mathbf{r}')\mathbf{E}_\eta(\mathbf{r}') \\
&= \sum_\lambda C_\lambda(\omega)\rho_{\lambda\xi}(\mathbf{r})^* \int \mathrm{d}r' \rho_\lambda(\mathbf{r}') \cdot \mathbf{E}(\mathbf{r}', \omega)
\end{aligned}$$

Therefore

$$\mathbf{P}_r(\mathbf{r}) = \sum_\lambda C_\lambda(\omega)\rho_\lambda(r)^* \int dr' \rho_\lambda(r') \cdot \mathbf{E}(\mathbf{r}', \omega) \tag{3.1.14}$$

Plug Eq. (3.1.14) into (3.1.11), we obtain

$$\mathbf{E}(\mathbf{r}) = \mathbf{E}_0(\mathbf{r}) + \sum_\lambda C_\lambda(\omega) \int \mathrm{d}r' \int dr'' G(\mathbf{r}, \mathbf{r}') \cdot \rho_\lambda(\mathbf{r}')^* \rho_\lambda(\mathbf{r}'') \cdot \mathbf{E}(\mathbf{r}'', \omega) \tag{3.1.15}$$

The inner products of Eq. (3.1.15) with $\rho_\lambda(\mathbf{r})$ integrated over $\mathbf{r}$ lead to the following linear algebraic equations as

$$(E_\lambda - h\omega - i\delta^+)F_\lambda + \sum_{\lambda'} A_{\lambda\lambda'}F_{\lambda'} = F^0_\lambda \tag{3.1.16}$$

with $F_\lambda = \dfrac{1}{E_\lambda - h\omega - i\delta^+} \int \mathrm{d}r \rho_\lambda(\mathbf{r}) \cdot \mathbf{E}(\mathrm{r})$, $F_\lambda^0 = \int \mathrm{d}r \rho_\lambda(\mathbf{r}) \cdot \mathbf{E}_0(\mathbf{r})$ and

$$A_{\lambda\lambda'} = -\int \mathrm{d}r \int \mathrm{d}r' \rho_\lambda(\mathbf{r}) \cdot G(\mathbf{r}, \mathbf{r}') \cdot \rho_{\lambda'}(r')^* \, .$$

As described in the linear equation system Eq. (3.1.16) in the problem of radiation-matter interaction, we have to deal with the coexisting electromagnetic field and charged particles. The problem is formulated as a scattering process. To compute F_λ^0 an eigenvalue problem of Schrödinger equation must be solved, then an integral must be carried out over the extension of the wavefunction. Once the initial condition F_λ^0 is given Eq. (3.1.16) could be solved. Finally the field $\mathbf{E}(\mathbf{r})$ is obtained by solving an integro-equation. This is a rather complicated process. In [12] the nonlocal response theory is formulated in a different way from what is discussed above. In fact, Maxwell's equations are given in terms of vector and scalar potentials, $\mathbf{A}$ and ϕ, respectively

$$\begin{cases} \nabla^2\phi + \frac{1}{c}\nabla \cdot \frac{\partial \mathbf{A}}{\partial t} = -4\pi\rho \\ \nabla^2 A - \frac{1}{c^2}\frac{\partial^2 \mathbf{A}}{\partial t^2} - \nabla(\nabla \cdot A + \frac{1}{c}\frac{\partial \phi}{\partial t}) = -\frac{4\pi}{c}\mathbf{j} \end{cases} \tag{3.1.17}$$

with

$$\mathbf{E} = \frac{1}{c}\frac{\partial \mathbf{A}}{\partial t} - \nabla\phi \, , \mathbf{H} = \nabla \times \mathbf{A} \, .$$

It can be verified that Maxwell's equations in potential forms (3.1.17) are invariant

under the following transformations

$$\begin{cases} \phi' = \phi - \frac{1}{c}\frac{\partial G}{\partial t} \\ \mathbf{A}' = \mathbf{A} + \nabla G \,, \end{cases}$$

where G is an arbitrary and well-behaved function called the gauge function or gauge operator. Maxwell's equations (3.1.17) enjoy the full gauge freedom. However, a particular gauge may be chosen with an appropriate choice of the gauge function. For example, a gauge transformation can always be made on the potential so that the Lorenz gauge condition is satisfied,

$$0 = \nabla \cdot \mathbf{A}' + \frac{1}{c}\frac{\partial \phi'}{\partial t} = \nabla \cdot \mathbf{A} + \nabla^2 G + \frac{1}{c}\frac{\partial \phi}{\partial t} - \frac{1}{c}\frac{\partial^2 G}{\partial t^2} \,. \tag{3.1.18}$$

Another choice is Coulomb gauge, which leads to the equation of motion

$$0 = \nabla \cdot \mathbf{A}' = 0 = \nabla \cdot \mathbf{A} + \nabla^2 G \,.$$

With Coulomb gauge being used in [12], we can easily solve for ϕ

$$\phi(\mathbf{r}, t) = \int \frac{1}{|\mathbf{r} - \mathbf{r}'|}\rho(\mathbf{r}', t)\mathrm{d}r' \,. \tag{3.1.19}$$

In terms of this result and consider the Fourier component of . ent of the the first

equation in (3.1.17) can be rewritten as

$$-(\nabla^2 + q^2)\mathbf{A}(\mathbf{r},\omega) = \frac{4\pi}{c}\mathbf{j}(\mathbf{r},\omega) + \frac{1}{c}\int \frac{\nabla'\nabla' \cdot \mathbf{j}(\mathbf{r}',\omega)}{|\mathbf{r}-\mathbf{r}'|} , \tag{3.1.20}$$

where a partial integration has been carried out in the integral and $q = \frac{\omega}{c}$ is the wavenumber in free space. Defining the Green function G_q satisfying the equation

$$(\nabla^2 + q^2)G_q(\mathbf{r},\omega) = -4\pi\delta(\mathbf{r}) ,$$

we can easily write down the solution of (3.1.20) as

$$\begin{aligned} \mathbf{A}(\mathbf{r}) = \mathbf{A}_0(\mathbf{r}) \;&+\; \frac{1}{c}\int G_q(\mathbf{r}-\mathbf{r}')\mathbf{j}(\mathbf{r}')\mathrm{d}r' \\ &+\; \frac{1}{4\pi c}\int \mathrm{d}r' \int \mathrm{d}r'' G_q(\mathbf{r}-\mathbf{r}')\frac{\nabla''\nabla'' \cdot \mathbf{j}(\mathbf{r}'',\omega)}{|\mathbf{r}'-\mathbf{r}''|} , \end{aligned}$$

where the argument ω is omitted for simplicity and $\mathbf{A}_0$ is the free field, usually corresponding to an incident field. Here the vector potential $\mathbf{A}$ is expressed as a functional of current density $\mathbf{j}$

$$\mathbf{A}(\mathbf{r}) = \mathbf{A}_0 + \mathcal{G}[\mathbf{j}] \tag{3.1.21}$$

with

$$\mathcal{G}[\mathbf{j}] \;=\; \frac{1}{c}\int G_q(\mathbf{r}-\mathbf{r}')\mathbf{j}(\mathbf{r}')\mathrm{d}r'$$

$$+\frac{1}{4\pi c}\int \mathrm{d}r' \int \mathrm{d}r'' G_q(\mathbf{r}-\mathbf{r}')\frac{\nabla''\nabla''\cdot\mathbf{j}(\mathbf{r}'',\omega)}{|\mathbf{r}'-\mathbf{r}''|} .$$

Next a functional $\mathbf{j}$ of $\mathbf{A}$ will be established from the first principle. The general Hamiltonian for an assemble of charged particles in a given electromagnetic radiation is:

$$H_M = \sum_l \{\frac{1}{2m_l}(p_l - \frac{e_l}{c}\mathbf{A}(r_l,t))^2 + e_l r_l \cdot \nabla\phi(r_l,t) + V(r_l)\} ,$$

Where the e_l, m_l, r_l and p_l are the charge, mass, coordinate and conjugate momentum of the coordinate, respectively, for the lth particle. And

$$H_0 = \sum_l \{\frac{1}{2m_l}p_l^2 + V(r_l)\}$$

$$H_{int} = \sum_l \frac{e_l^2}{2m_l c^2}\mathbf{A}^2 - \frac{e_l}{m_l c}p_l \cdot \mathbf{A} + e_l r_l \cdot \nabla\phi$$

are regarded as the unperturbed Hamiltonian and the interaction Hamiltonian, respectively. The Schrödinger equation governs the time evolution of wavefuvntion Ψ

$$i\hbar\frac{\partial}{\partial t}\Psi(\mathbf{r},t) = \hat{H}_M\Psi(\mathbf{r},t) .$$

Without giving the detailed derivation we write down the final expression

$$\mathbf{j}(\mathbf{r},t) = \langle\Psi|\hat{\mathbf{J}}|\Psi\rangle = \mathcal{F}(\mathbf{A}) , \qquad (3.1.22)$$

where

$$\hat{\mathbf{J}} = \hat{\mathbf{I}} - \sum_l \frac{e_l^2}{m_l c}\mathbf{A}(\mathbf{r},t)\,,$$
$$\hat{\mathbf{I}} = \sum_l \frac{e_l}{2m_l}[p_l\delta(\mathbf{r}-\mathbf{r_l}) + \delta(\mathbf{r}-\mathbf{r_l})p_l].$$

So we have the functional relationships between the induced current density $\mathbf{j}(\mathbf{r},t)$ and the vector potential $\mathbf{A}(\mathbf{r},t)$ as

$$\mathbf{j}(\mathbf{r},t) = \mathcal{F}[\mathbf{A}]\,,$$
$$\mathbf{A}(\mathbf{r},t) = \mathbf{A_0}(\mathbf{r},t) + \mathcal{G}[\mathbf{j}]\,.$$

The former is obtained from the solution of the Schrödinger equation for a given vector potential and the latter from the Maxwell equations for a given current density. These two equations for $\mathbf{A}$ and $\mathbf{j}$ should be solved simultaneously. Indeed, by specifying the initial condition both $\mathbf{j}$ and $\mathbf{A}$ can be calculated at any $(\mathbf{r},t)$. Reader is referred to chapter 2 of [12] for for detailed formulation of the approach.

In addition to Cho's nonlocal microscopic response theory, there are two types of approaches by the groups of Keller [32] and Stahl [58] worth to mention. They both take the coherence of matter-excited states into account in calculating the linear and nonlinear optical responses of various forms of mater within the semiclassical scheme. Keller's method is rather similar to Cho's approach; Two integral equations for electromagnetic field and transition current density. Stahl's coherent wave approach uses

"interband transition amplitudes" to set up the constitutive equation between the interband current density and electric field.

Inspired by Cho's work and based on understanding the nonlocality nature of nano optical responses, a different semiclassical model is developed. It should be pointed out that only the transverse component of the electromagnetic fields and full Coulomb interaction among particles are included in the matter Hamiltonian. However, a different Hamiltonian is used in our model. For the matter Hamiltonian (unperturbed Hamiltonian) only the kinetic energy and Couloumb interaction of charged particles are included, and for the matter-light interaction Hamiltonian, we take the full EM field as the external field. By using the dipole moment approximation and introducing the electric dipole operator, we are able to write the matter-light interaction Hamiltonian (perturbed part) into an integral form. After these initial steps, we derive a formula for the calculation of the susceptibility, then a new dielectric constant which depends on the wavevector as well as frequency. The model is applied to study various problems related to exctions and biexcitons confined in nanoscale semiconductors.

3.2 Dielectric constant

In this part a new dielectric constant will derived from the first principle. Starting from the microscopic Maxwell's equation (2.1.5) and nonlocal polarization (3.1.7), a new Hamiltonian for an assemble of charged particles in an applied electromagnetic

radiation is introduced to read

$$H_M = H_0 + H_{int} ,$$

which is written as the sum of the Hamiltonian H_0 for the matter system and an interaction Hamiltonian, H_{int}, which describes the interaction of the matter with the electromagnetic field. Usually, we take them to be the following forms [10]

$$H_0 = \sum_l \left\{ \frac{1}{2m_l} \mathbf{p}_l^2 + V(\mathbf{r}_l) \right\} ,$$

$$H_{int} = -\sum_l e_l \mathbf{r}_l \cdot \mathbf{E}(\mathbf{r}_l, t) , \tag{3.2.1}$$

where e_l, m_l, $\mathbf{r}_l$ and $\mathbf{p}_l$ are the charge, mass, coordinate and conjugate momentum of the coordinate, respectively, for the lth particle, $V(\mathbf{r}_l)$ is the Couloumb interaction of charged particles. We assume that $\mathbf{E}(\mathbf{r}, t)$ can be represented as a discrete sum of (positive and negative) frequency component as

$$\mathbf{E}(\mathbf{r}, t) = \sum_\omega \tilde{\mathbf{E}}(\mathbf{r}, \omega) \exp(-i\omega t) .$$

So (3.2.1) can also be written as $-\sum_\omega \int d\mathbf{r} \hat{\mathbf{P}}(\mathbf{r}) \cdot \tilde{\mathbf{E}}(\mathbf{r}, t) \exp(-i\omega t)$, where $\hat{\mathbf{P}}(\mathbf{r}) = \sum_l e_l \mathbf{r} \delta(\mathbf{r} - \mathbf{r}_l)$ is the electric dipole moment operator. The time evolution of matter

state is described by the Schrödinger equation

$$i\hbar\frac{\partial}{\partial t}|\psi(t)\rangle = (H_0 + H_{int})|\psi\rangle \ . \tag{3.2.2}$$

The matter state prepared at time $t = t_0$ as an eigenstate of H_0 will experience time evolution after switching on the radiation-matter interaction.

The susceptibility tensor with respect to the induced polarization can be derived from the conventional time-dependent perturbation theory.

By introducing $|\hat{\psi}(t)\rangle = \exp(iH_0t/\hbar)|\psi(t)\rangle$, Equation (3.2.2) can be rewritten as

$$i\hbar\frac{\partial}{\partial t}|\hat{\psi}(t)\rangle = \hat{H}|\hat{\psi}\rangle \tag{3.2.3}$$

with

$$\hat{H} = \exp(iH_0t/\hbar)H_{int}\exp(-iH_0t/\hbar) \ .$$

Solving Equation (3.2.3) up to the first-order of $\hat{H}$, we have

$$|\hat{\psi}(t)\rangle = |\hat{\psi}(-\infty)\rangle - \frac{i}{\hbar}\int_{-\infty}^{t} d\tau\hat{H}(\tau)|\hat{\psi}(-\infty)\rangle \ .$$

By assuming that the matter is in the ground state $|g\rangle$ at $t = -\infty$, the first-order perturbed states are given by

$$|\hat{\psi}(t)\rangle \ = \ |g\rangle \ - \frac{i}{\hbar}\sum_{\omega}\sum_{\xi}|\xi\rangle\int_{-\infty}^{t} d\tau e^{i(E_\xi/\hbar-\omega-i\gamma/\hbar)\tau}\langle\xi|\left[-\int d\mathbf{r}'\hat{\mathbf{P}}(\mathbf{r}')\cdot\tilde{\mathbf{E}}(\mathbf{r}')\right]|g\rangle$$

$$= |g\rangle - \sum_{\omega}\sum_{\xi}|\xi\rangle\frac{\langle\xi| - \int d\mathbf{r}'\hat{\mathbf{P}}(\mathbf{r}')\cdot\tilde{\mathbf{E}}(\mathbf{r}')|g\rangle}{E_\xi - \hbar\omega - i\gamma}e^{i(E_\xi/\hbar-\omega-i\gamma/\hbar)t},$$

where a factor $\exp(\frac{\gamma}{\hbar}\tau)$, $\gamma \to 0^+$ is introduced to indicate that at time $t_0 \to -\infty$, the perturbation H_{int} is turned on adiabatically. This factor serves mainly the purpose of keeping the derivation of all mathematical quantities properly behaved, i.e., non-singular. Here, E_ξ indicates the eigenenergy of excited state $|\xi\rangle$ measured from that of the ground state $|g\rangle$.

The expectation value of the polarization can be calculated as

$$\begin{aligned}
\mathbf{P}(\mathbf{r},t) &= \langle\hat{\psi}(t)|e^{iH_0t/\hbar}\hat{\mathbf{P}}(\mathbf{r})e^{-iH_0t/\hbar}|\hat{\psi}(t)\rangle \\
&= -\sum_{\omega}\sum_{\xi}\langle g|\hat{\mathbf{P}}(\mathbf{r})|\xi\rangle\frac{\langle\xi| - \int d\mathbf{r}'\hat{\mathbf{P}}(\mathbf{r}')\cdot\tilde{\mathbf{E}}(\mathbf{r}')|g\rangle}{E_\xi - \hbar\omega - i\gamma}e^{-i\omega t}e^{(\gamma/\hbar)t} \\
&\quad -\sum_{\omega}\sum_{\xi}\langle\xi|\hat{\mathbf{P}}(\mathbf{r})|g\rangle\frac{\langle g| - \int d\mathbf{r}'\hat{\mathbf{P}}(\mathbf{r}')\cdot\tilde{\mathbf{E}}(\mathbf{r}')|\xi\rangle}{E_\xi - \hbar\omega + i\gamma}e^{i\omega t}e^{(\gamma/\hbar)t}.
\end{aligned}$$

Then the Fourier component $\tilde{\mathbf{P}}(\mathbf{r})$ may be written as

$$\tilde{\mathbf{P}}(\mathbf{r}) = \sum_{\xi}\langle g|\hat{\mathbf{P}}(\mathbf{r})|\xi\rangle\frac{\langle\xi|\int d\mathbf{r}'\hat{\mathbf{P}}(\mathbf{r}')\cdot\tilde{\mathbf{E}}(\mathbf{r}')|g\rangle}{E_\xi - \hbar\omega - i\gamma} + \sum_{\xi}\langle\xi|\hat{\mathbf{P}}(\mathbf{r})|g\rangle\frac{\langle g|\int d\mathbf{r}'\hat{\mathbf{P}}(\mathbf{r}')\cdot\tilde{\mathbf{E}}(\mathbf{r}')|\xi\rangle}{E_\xi + \hbar\omega + i\gamma}. \tag{3.2.4}$$

By ignoring the second term of Equation (3.2.4) that corresponds to the antiresonant part, the induced polarization takes the form

$$\tilde{\mathbf{P}}(\mathbf{r}) = \int d\mathbf{r}'\chi(\mathbf{r},\mathbf{r}')\cdot\tilde{\mathbf{E}}(\mathbf{r}',\omega)$$

with $\chi(\mathbf{r}, \mathbf{r}'; \omega)$ being the susceptibility tensor

$$\chi(\mathbf{r}, \mathbf{r}'; \omega) = \sum_{\xi} \frac{\langle g|\hat{\mathbf{P}}(\mathbf{r})|\xi\rangle\langle\xi|\hat{\mathbf{P}}(\mathbf{r}')|g\rangle}{E_{\xi} - \hbar\omega - i\gamma} .$$

In the case of bulk materials, the center of mass-motion of the exciton is approximately represented by a plane wave [4]

$$\langle g|\hat{\mathbf{P}}(\mathbf{r})|\xi\rangle = \frac{\boldsymbol{\mu}}{\sqrt{V}} \exp(i\mathbf{k}\cdot\mathbf{r}) , \tag{3.2.5}$$

where ξ represents the exciton state with the wave vector $\mathbf{k}$, V is the volume of the medium, and $\boldsymbol{\mu}$ is the intensity of induced polarization obtained from the bulk limit, $\boldsymbol{\mu}^2 = \frac{\epsilon_{bg}\Delta_{LT}}{4\pi}$, and Δ_{LT} is the splitting energy of longitudinal and transverse mode of exciton, ϵ_{bg} is the background dielectric constant.

From (3.2.5), it follows that

$$\chi(\mathbf{r}, \mathbf{r}') = \frac{\boldsymbol{\mu}^2}{V} \sum_{\mathbf{k}} \frac{e^{i\mathbf{k}\cdot(\mathbf{r}-\mathbf{r}')}}{E_{\mathbf{k}} - \hbar\omega - i\gamma} = \chi(\mathbf{r} - \mathbf{r}') . \tag{3.2.6}$$

When the valence and conduction bands are both parabolic in the $\mathbf{k}-$region, the energy of the exciton may be further given by

$$E_{\mathbf{k}} = E_0 + \frac{\hbar^2\mathbf{k}^2}{2M} ,$$

where $E_0 = \hbar\omega_0$, and M is the mass of the exciton.

Next, define the Fourier component in the $\mathbf{k}-$space of the susceptibility

$$\chi(\mathbf{r}-\mathbf{r}') = \frac{1}{\sqrt{V}}\sum_{\mathbf{k}} e^{i\mathbf{k}\cdot(\mathbf{r}-\mathbf{r}')}\chi(\mathbf{k}) \,,$$

then we have

$$\chi(\mathbf{k}) = \frac{1}{\sqrt{V}}\frac{\boldsymbol{\mu}^2}{E_0 + \frac{\hbar^2\mathbf{k}^2}{2M} - \hbar\omega - i\gamma} \,.$$

Since the polarization induced by the exciton is $\tilde{\mathbf{P}}(\mathbf{r}) = \int d\mathbf{r}'\chi(\mathbf{r},\mathbf{r}',\omega)\cdot\tilde{\mathbf{E}}(\mathbf{r}',\omega)$,

we can rewrite this relation in the $\mathbf{k}-$space as

$$\begin{aligned}\frac{1}{\sqrt{V}}\sum_{\mathbf{k}}\mathbf{P}(\mathbf{k}) &= \int d\mathbf{r}'\frac{1}{\sqrt{V}}\sum_{\mathbf{k}'} e^{i\mathbf{k}'\cdot\mathbf{r}'}E_\omega(\mathbf{k}')\cdot\frac{1}{\sqrt{V}}\sum_{\mathbf{k}} e^{i\mathbf{k}\cdot(\mathbf{r}-\mathbf{r}')}\chi(\mathbf{k}) \\ &= \sum_{\mathbf{k}} e^{i\mathbf{k}\cdot\mathbf{r}}\chi(\mathbf{k})\cdot E_\omega(\mathbf{k}) \,,\end{aligned}$$

where we used the fact $\frac{1}{V}\int d\mathbf{r}\exp(-i\mathbf{k}'\cdot\mathbf{r})\exp(i\mathbf{k}\cdot\mathbf{r}) = \delta_{\mathbf{k},\mathbf{k}'}$. Hence, $\bar{\chi}(\mathbf{k},\omega)$ may be defined as follows:

$$\bar{\chi}(\mathbf{k},\omega) = \sqrt{V}\chi(\mathbf{k};\omega) = \frac{\boldsymbol{\mu}^2}{E_0 + \frac{\hbar^2\mathbf{k}^2}{2M} - \hbar\omega - i\gamma} \,.$$

The new dielectric constant takes the form

$$\varepsilon(\mathbf{k},\omega) = \varepsilon_b + 4\pi\bar{\chi}(\mathbf{k},\omega) = \epsilon_b + \frac{\varepsilon_b\Delta_{LT}}{E_0 + \frac{\hbar^2\mathbf{k}^2}{2M} - \hbar\omega - i\gamma} \,, \tag{3.2.7}$$

which depends explicitly on the wavevector $\mathbf{k}$ and the frequency ω. It should be

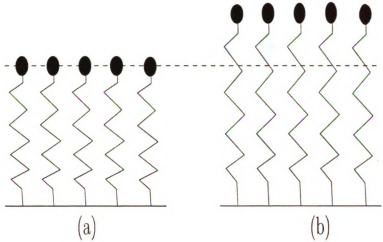

Figure 3.3: Uncoupled oscillators (electrons attached to nuclei via springs) in their equilibrium position (a); elongated with a incident light (b).

noted that this dielectric constant applies to a case in which the exciton polarization and the electric field are parallel, and both perpendicular to $\mathbf{k}$ [28]. In general, the wavevector dependence of the dielectric constant is referred to as spatial dispersion for which Hopfield and Thmoas did a systematical study in [28]. Indeed the nonlocal effect of the optical response is implicitly contained in the dielectric constant (3.2.7), and there is an intuitive physical interpretation. Take the Lorentz model as an example, we have assumed zero coupling between neighboring electrons (oscillators) as shown in Fig. (3.3). The spatial nonlocal effects from the neighboring oscillators are not considered in Lorentz model. However, a more realistic coupling between the neighboring oscillators, or nonlocal response effect, is contained in the wavevector-dependence dielectric constant (3.2.7). As illustrated in Fig. (3.4), the neighboring oscillators are coupled via weak springs. The most important consequence is that the eigenfrequency is now function of k, namely $\omega_0'(k) = \omega_0 + \frac{\hbar \mathbf{k}^2}{2M}$. For incident light, the coupling springs are elongated and increase the "effective" spring constant. As a

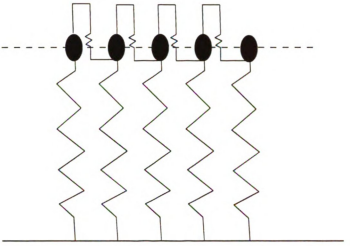

Figure 3.4: An ensemble of coupled oscillators.

consequence, the eigenfrequency increases with increasing k. For our model system, this is also true for excitons whose effects will be discussed later on. The fact that the eigenfrequency ω_0' of some excitation of a solid depends on k is often called "spatial dispersion". The development of the spatial dispersion in optical spectra of excitons has in great part been due to Pekar [49], Hopfield and Thomas [28].

3.2.1 Exctions and biexctions

In this part the dielectric constant (3.2.7) will be employed to model the excitons and biexcitons effects in nanocrystals. Some definitions and concepts will be briefly introduced at first. [23, 33] are very good references for a thorough study on excitons and biexcitons. A paper [36] by Liang also provides some fundamentals on excitons.

An exciton is a bound state of an electron-hole pair in semiconductors. To visualize the formation of excitons consider the simplest two-band model [23], the electrons are accumulated at lower band (valence band) and the higher band (conduction band)

is empty. Electrons can be moved from valence to conduction band by an electromagnetic field having the energy comparable to the band gap, and meanwhile positively charged holes are left in the valence band. The electron and the hole form a pair by attracting each other via Coulomb force, this electron-hole pair is called exciton. Furthermore, the interactions between excitons should be taken into account if large density of excitons is created in a material. Provided that the interaction is attractive, two excitons could bind to form a biexciton. A great deal of research has been devoted to the study of the exciton effects since the concept of exciton was first introduced by Frenkel in 1931 [21]. The fundamental importance of the excitons in semiconductors is clear. They are found to be playing an essential role in optical effects such as luminescence, fluorescence, photographic process, photoconductivity, and so on [36]. These various features enable semiconductors to be widely used in numerous fields, including optical communication, computing, biomedical imaging, and data storage. The electric and optical properties of excitons in bulk semiconductors have been extensively studied (see Chap. 13 of [33] and references therein). For the excitons in structures of reduced dimensionality, for example, in nanoscale structures such as quantum well, quantum wire and quantum dot, the states of the exciton shift to higher energy as the size of structure decreases. This situation is called quantum confinement effect, which makes nanoscale semiconductor cease to resemble bulk, exhibits strikingly different properties instead [50, 66]. For example, Hanamura showed in [24] theoretically that the nonlinear optical polarisability can

be enhanced greatly in semiconductor microcrystallites where the exciton becomes quantized due to the confinement. His calculation suggested that in case of CuCl microcrystal of size about 6.4 nanometer, an enhancement of the order of 10^4 for $\chi^{(3)}$ can be expected; Recently the study ultra-efficient solar cells has been attracted a great deal of research efforts, Quantum dots are offering the possibilities for improving the efficiency of solar cells in at least two respects, by extending the band gap of solar cells for harvesting more of the light in the solar spectrum,and by generating more charges from a single photon [17]. Therefore, as the size of a semiconductor is getting smaller, excitons and exciton-biexciton coupling inside are no more minor perturbation as in the comparable bulk system, but actually play a very important role in defining the optical properties.

For simple parabolic bands and direct-gap semiconductors one can separate the relative motion of electron and hole and the motion of the center of mass. Usually, the motion of an exciton is quite different in two limiting situations characterized by the ratio of the system's size L to the effective Bohr radius a_B of the exciton in bulk material [4]. Therefore, we have two cases, **a)** $L \gg a_B$ (weak confinement regime). In this limit the size quantization of the exciton is brought about, and the e-h relative motion stays almost as in the bulk material and only the center-of-mass motion is affected by the confinement; **b)** $L \ll a_B$ (strong confinement regime). This is opposite to case a), the size quantization effect of the electron and hole is much larger than the exciton effect, the energy of an exciton is mainly determined by the individual size

quantization with a small correction due to the Coulomb interaction. The dissertation concerns the first case in which the internal structure of the exciton remains nearly the same as in the bulk, but its motion is quantized due to the confinement. Then the energy of the exciton E_{ex} in nanocrystals include two parts: $E_g = \hbar\omega_0$ which is the energy for overcoming the bandgap; $\frac{\hbar^2 k^2}{2M}$ is the kinetic energy possessed by the exciton. Hence the nonlocal exciton effects on the optical properties is contained in the $k-$dependent dielectric constant (3.2.7). In comparison, the classical dielectric theory of optical properties studies the dielectric constant depending only on the frequency. The dielectric behavior is a sum over resonances, each resonance occurring at a particular frequency. Moreover, the transport of energy is neglected by any mechanism other than electromagnetic waves. However, we are investigating the optical response of confined excitons in a nano medium, so the energy transports by excitons and the electromagnetic field are equally important.

Exciton is an elementary excitation, or quasiparticle of a semiconductor. In current research, the bound electron and hole pairs (excitons) provide a means to transport energy without transporting net charge [36]. Since an exciton is a bound state of an electron and a hole, the overall charge for this quasiparticle is zero. Hence it carries no electric current. Under certain conditions two excitons could bind to form a new quasiparticle, the so called biexciton or exciton molecule [35]. The exciton to biexciton transition in nanostructures has been observed and studied by many groups, and some resonance phenomena, e.g., electromagnetic induced transparency, were re-

ported in [7, 9, 11]. The nonlinear optical response of biexciton in semiconductors has been studied recently by several groups in relation to its potential applications in optical bistability. Three different approaches have been proposed to solve this problem: Green functions [39], Bloch equations [26] and unitary transformation [1–3]. In [39] the author derived a non-perturbative expression of nonlinear dielectric constant of the exciton-biexciton transition

$$\varepsilon(\omega) = \varepsilon_{\mathrm{b}} + 4\pi\mu_{\mathrm{gx}}^2 G_{\mathrm{x}}(\omega) \,, \tag{3.2.8}$$

where $G_{\mathrm{x}}(\omega) = \dfrac{1}{\omega_{\mathrm{ex}} - \omega + i\gamma + \Sigma}$ is the renormalized Green function with the dynamical self-energy $\Sigma = \dfrac{\mu_{\mathrm{xb}}^2 |E|^2}{\omega_{\mathrm{bi}} - 2\omega + i\beta}$ which represents the contribution to the exciton's energy due to the interactions between the excitons and the system it is part of. Here ε_{b} is the background dielectric constant of the medium and assumed to be homogeneous, μ_{gx} and μ_{xb} are the transition probabilities from ground state to the exciton state (frequency ω_{ex}) and from the exciton to the biexciton state (frequency ω_{bi}), respectively. γ and β are damping constants.

Based on understanding the $k-$dependence and inspired by the expression (3.2.8), a modified dielectric function of exciton-biexciton coupling can be obtained by adding the wavevector

$$\varepsilon(k,\omega) = \varepsilon_{\mathrm{b}} + \frac{4\pi\mu_{\mathrm{gx}}^2}{\omega_{\mathrm{ex}} - \omega + \frac{\hbar k^2}{2M} + i\gamma + \Sigma_k} \,, \tag{3.2.9}$$

where a $k-$dependent self-energy $\Sigma_k = \dfrac{\mu_{\mathrm{xb}}^2 |E|^2}{\omega_{\mathrm{bi}} - 2\omega + \frac{\hbar k^2}{M} + i\beta}$ is obtained. The effec-

tive mass of the biexciton is assumed to be just twice that of the exciton. The energy of the biexciton is given by $E_{\rm bi} = \hbar\omega_{\rm bi} + \frac{\hbar^2 k^2}{M}$, and the wavevector of the biexciton is assumed to be $2k$ which is twice that of the exciton.

The formation of a biexciton is essentially due to the two-photon absorption resonance. Physically the biexciton can be produced under several different situations. For example, two excitons interact with each other to form a biexciton in a high dense excitonic system in which the dielectric function takes the form (3.2.9); Consider a system which is probed (by probe light ω) being disturbed by a pump light ($\omega_{\rm p}$). If the probe and pump light frequencies are both chosen in resonance with some of the transition energies of the system, then the optical property is modified to take a form which is similar to (3.2.9) with a different self-energy $\Sigma_k = \frac{\mu_{\rm xb}^2 |E_{\rm p}|^2}{\omega_{\rm bi} - \omega_{\rm p} - \omega + \frac{\hbar k^2}{M} + i\beta}$. Here $|E_{\rm p}|^2$ is the intensity of the applied pump light.

3.3 Finite-size effects

The nonlocal effects of optical responses of two-band nanocrystals is reflected in the wavevector-dependent dielectric constants. More realistically, finite-size effects have to be taken into account when studying the optical properties of nanocrystals. Finite-size effects, or sometimes called quantum confinement effects, have been observed for small colloidal CdS nanocrystal [51, 53] and semiconducting nanoparticles embedded in a glass matrix [16, 64]. In the early 1980s experiments were done with colloidal solutions of quantum dots with applications towards solar energy conversion and pho-

tocatalysis. It was found that colloidal solutions of the same semiconductor showed strikingly different colors when the size of the quantum dots was varied. This observation (called coloration) is attributed to the finite-size effect. Once the size of a nanocrystal approaches the limit of the Bohr radius of an exciton, the states of the exciton shift to higher energy as the confinement energy increases [46]. The confinement energy arises from the fact that according to the Heisenberg uncertainty principle the momentum of a particle increases if its position becomes well defined. In [24] Hannamura has made a theoretical study of the finite-size effects on the oscillator strength and third-order optical polarisability $\chi^{(3)}$ of nanocrystals. From an engineering point of view, material with a large optical nonlinearity is required for optical shutters or optical information processors. He showed that the extremely small scales of nanocrystals actually result in two major effects on their optical properties. One is the size quantization of excitons. The other is deviation of the electronic excitation from an ideal harmonic oscillator. In weak confinement regime the former effect is significant while the latter effect is less important. Hence the discussion will be centered on the size quantization of excitons.

In the limit of weak confinement the size quantization of the exciton is brought about. As in [24] consider first a cubic box containing N^3 unit cells. For the parabolic conduction and valence bands with effective masses m_e and m_h, respectively, the size quantization is governed by the relationship among the medium size $L = nu$, and the effective Bohr radius of electron $a_e = \hbar^2 \varepsilon_b / m_e e^2$ and hole $a_h = \hbar^2 \varepsilon_b / m_h e^2$, where

u is the length of the unit cell and ε_{b} is the background dielectric constant. The size quantization energies can be expressed for the electron and hole as

$$\Delta E_c = \frac{3\pi^2\hbar^2}{2m_eL^2}\,, \Delta E_v = \frac{3\pi^2\hbar^2}{2m_eL^2}\,.$$

The Coulomb interaction between the electron and the hole is

$$V_{\mathrm{exc}} = \frac{e^2}{\varepsilon_{\mathrm{b}}a} = \frac{e^2}{\varepsilon_{\mathrm{b}}(a_e + a_h)}\,,$$

where a is the Bohr radius of the exciton. The weak confinement condition $L \gg (a_e + a_h) = a$ is equivalent to $V_{\mathrm{exc}} \gg \Delta E_c + \Delta E_v$. In this case, the energy of the exciton in the box is

$$E_n = E_{\mathrm{g}} - E^b_{\mathrm{exc}} + \frac{\hbar^2\pi^2n^2}{2ML^2}\,, \tag{3.3.1}$$

where $E^b_{\mathrm{exc}} = \mu e^4/2\hbar^2\varepsilon^2_{\mathrm{b}}$ is the exciton binding energy, $\mu = m_em_h/(m_e + m_h), M = m_e + m_h$, and $n = (n_x, n_y, n_z)$. For the case of a quantum sphere with an infinite wall at $R \geq R_0$, the radius of the sphere, the energy of the optically allowed exciton is

$$E_{n00} = E_{\mathrm{g}} - E^b_{\mathrm{exc}} + \frac{\hbar^2\pi^2n^2}{2MR_0^2}\,.$$

The size-quantization effect on the absorption spectrum was observed in [51, 53] and theoretically studied in [16, 64]. In [24] the effect of very large oscillator strength was brought about for weak confinement case. Since the sum of the whole oscillator

strength is constant as long as the concentration of the medium is kept constant. Hence the oscillator strength is concentrated in the lower excitation states. Without giving details the expression for the oscillator strength per quantum box is given in [24] by

$$f_n = \frac{2m}{\hbar}\omega_n |p_{cv}|^2 \left[\frac{2\sqrt{2}}{\pi}\right] \frac{N^3}{(n_x n_y n_z)^2} .$$

And the result for a quantum sphere with $R_0 = uN$ is

$$f_{n00} = \frac{2m}{\hbar}\omega_n |p_{cv}\phi_{1s}(0)|^2 u^3 \frac{8N^3}{\pi n} .$$

Motivated by Hannamura's work on the finite-size effects several refinements to the wavevector-dependent dielectric constants need to be made. Most importantly, the exciton's energy (for the lowest excitation state) has to be modified $E_1 = \hbar\omega_0 - E^b + \frac{\hbar^2\mathbf{k}^2}{2M} + \frac{\hbar^2\pi^2}{2ML^2}$. The eigenfrequency of the exciton in the lowest excite state is $\omega_1 = \omega_0 - E^b/\hbar + \frac{\hbar\mathbf{k}^2}{2M}$. Hence the dielectric constant due to the excitons effect is changed to

$$\varepsilon(\mathbf{k},\omega) = \varepsilon_b + \frac{4\pi\mu^2}{\hbar\omega_1 - \hbar\omega - i\gamma} .$$

It is valid to use the bulk limit for μ in the weak confinement regime. However, the finite-size effects on the transition dipole moment have to be taken into account in order to obtain a more accurate model. For the one-dimensional confinement (quantum slab) the squared transition dipole moment $|\mu|^2$ is increased by the factor $E_1 8N/E_0\pi^2$, and it should be multiplied by the factor $E_1 8N^3/E_0\pi$ for a quantum

dot. In order to fully understand the structure of the electronic states in a semiconductor nanocrystal other effects, like the band-filling effect and the screening effects as well as exchange interaction between electrons and holes also need to be taken into account [44].

Chapter 4

MATHEMATICAL ANALYSIS

As we have discussed in previous chapters, some physicists have begun to address the challenging problems in modeling the optical interaction with nanostructures, the underlying mathematical analysis and numerical computation remain open. Initial attempts have been made recently in [5, 6, 59] during my doctoral study to deal with some mathematical issues arising from these problems which is also the central topic of this chapter.

4.1 Concept of polaritons

To better understand what is actually propagating when "light" travels through matter the concept of polariton has to be introduced. Simply speaking, polaritons are quasiparticles resulting from strong coupling of electromagnetic waves with an electric or magnetic dipole-carrying excitation. More details are going to be discussed [33].

In vacuum the light is a transverse electromagnetic wave, the quanta of which

are known as photons. To describe the interaction of light with matter one way is to treat the electromagnetic field and the excitations of the matter as independent quantities, this is called perturbative treatment or weak coupling. In this case a photon is absorbed and the matter goes from the ground state to the excited state, and that is it. It is sufficient to use this approach for many purposes, but, if we look closer, we find that this is not the whole story. The optically excited state of the matter is necessarily connected with some polarization $\mathbf{P}$. Otherwise the transition would be optically forbidden, i.e., it would not couple to the electromagnetic field e.g. via the dipole operator. On the other hand, every oscillating polarization emits an electromagnetic wave which may act back to onto the incident electromagnetic field. This interplay leads us to the strong coupling between light and matter and to the concept of polaritons which was first introduced for crystalline solids [28]. For our interest the discussion is centered on exciton-polariton, resulting from coupling of visible light with an exciton.

As mentioned earlier the term "dispersion relation" or simply "dispersion" means the relation $\omega(k)$ for all wave-like excitations independent of the functional dependence. It can be simply a horizontal line, a linear or parabolic relation, or something more complicated. Every excitation which has a wave-like character has a dispersion relation. For the exciton-polariton (from now on we use polariton without causing confusion) to determine the its dispersion relation, we must combine the polariton equation $\frac{c^2k^2}{\omega^2} = \varepsilon$ with the dielectric function $\varepsilon(k,\omega)$. For the new spatially disper-

sive dielectric constant (3.2.7) due to the exciton effects, the polariton's dispersion relation is

$$\frac{c^2k^2}{\omega^2} = \varepsilon_b + \frac{4\pi\mu^2}{\hbar\omega_0 + \frac{\hbar^2\mathbf{k}^2}{2M} - \hbar\omega - i\hbar\gamma} .$$

Or

$$k^4 + \left[\frac{2M}{\hbar}(\omega_0 - \omega - i\gamma) - \epsilon_{bg}q^2\right]k^2 - \epsilon_{bg}q^2\frac{2M}{\hbar}(\omega_0 - \omega - i\gamma + \Delta_{LT}/\hbar) = 0 , \quad (4.1.1)$$

where $\varepsilon_b\Delta_{LT} = 4\pi\mu^2$. It can be easily seen that Eq. (4.1.1) leads to four complex solutions and two of them k_1, k_2 with positive imaginary parts corresponding to physically meaningful hence acceptable modes. It means that in a medium characterized by (3.2.7) there are two propagating waves (polariton modes), which is a striking property of such medium.

Similarly, for an exciton-biexciton coupling medium described by (3.2.9) the dispersion relation

$$k^6 + a(\omega)k^4 + b(\omega)k^2 + c(\omega) = 0 \quad (4.1.2)$$

with

$$\begin{aligned}
a(\omega) &= \frac{M}{\hbar}(\omega_{\rm bi} - \omega_{\rm pu} + 2\omega_{\rm ex} - 3\omega - i\beta - i2\gamma) - \left(\frac{\omega}{c}\right)^2\varepsilon_{\rm b} , \\
b(\omega) &= \frac{M}{\hbar}(\omega_{\rm bi} - \omega_{\rm pu} - \omega - i\beta)\left[\left(\frac{\omega}{c}\right)^2\varepsilon_{\rm b} + \frac{2M}{\hbar}(\omega_{\rm ex} - \omega - i\gamma)\right] - \frac{8\pi M}{\hbar^2}\mu_{\rm gx}^2\left(\frac{\omega}{c}\right)^2 \\
&\quad -\frac{2M}{\hbar}\left(\frac{\omega}{c}\right)^2\varepsilon_{\rm b}(\omega_{\rm ex} - \omega - i\gamma) + \mu_{\rm xb}^2|E_0|^2\frac{2M^2}{\hbar^4} , \\
c(\omega) &= \frac{2M^2}{\hbar^2}\left[\frac{\mu_{\rm xb}^2|E_0|^2}{\hbar^2} + (\omega_{\rm bi} - \omega_{\rm pu} - \omega - i\beta)(4\pi\mu_{\rm gx}^2/\hbar + \varepsilon_{\rm b}(\omega_{\rm ex} - \omega - i\gamma))\right]\left(\frac{\omega}{c}\right)^2 .
\end{aligned}$$

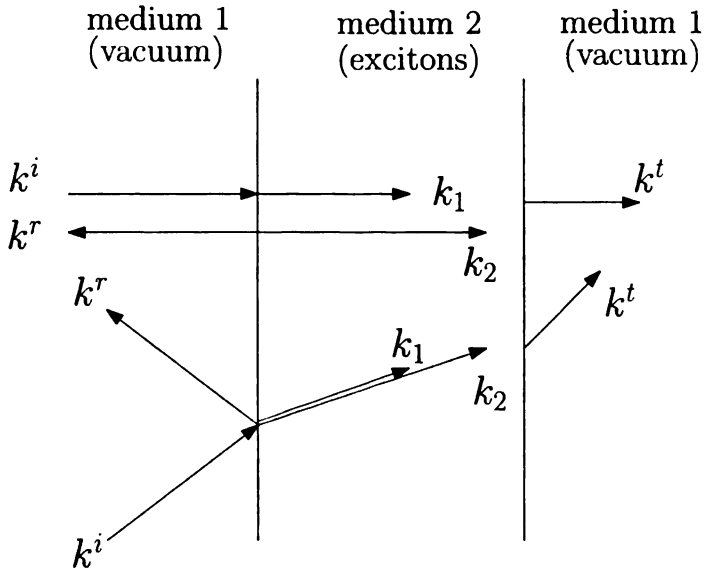

Figure 4.1: Two waves in a semiconducting nano slab which confines excitons.

It can be verified that the above equation has six complex roots, and three of them k_1, k_2 and k_3 with positive imaginary parts corresponding to physically meaningful hence acceptable modes.

It can be seen when the exciton/biexciton medium characterized by (3.2.7)/(3.2.9) is irradiated with light of frequency ω, more than one waves can arise inside the medium with the same frequency but with different wavenumbers. Therefore, the need of additional boundary conditions (abc) arise naturally to handle the multi-mode waves.

4.2 Additional boundary conditions

To make the situation clear, we show in Fig. 4.1 the wavevectors for such cases for normal and oblique incidence. The incident and reflected beams obeys the usual law of reflection, their composition parallel to the surface are equal. The same is true

for the transmitted beams. As mentioned the abc is required to handle the multiple waves inside the medium, although the abc can not be deduced from Maxwell's equations. Their capacity is exhausted with the continuity of the tangential components of fields on the interface. Since the complex index of refraction around the resonance is different for the k_1 and k_2 branch, which therefore contribute differently to the reflection and transmission spectra, the abc should contain information about the "branching ratio", i.e., which fractions of the incident beam couple in the medium to the k_1 branch and to the k_2 branch as a function of frequency.

The abc are based mainly on arguments of physical plausibility. On the vacuum side of the interface in Fig. 4.1 the polarization induced by excitons is zero since the excitons are not allowed to escape from inside the medium. To avoid an unphysical discontinuity in the polarization, we propose that the tangential component of the polarization should vanish at the interface

$$\mathbf{n} \times \mathbf{P} = 0 \,. \tag{4.2.1}$$

Another argument says that the polarization should vary smoothly across the interface, implying that the derivation with respect to the normal direction has to be zero, resulting in

$$\frac{\mathrm{d}\mathbf{P}}{\mathrm{d}\mathbf{n}} = 0 \,. \tag{4.2.2}$$

Sometimes a linear combination of (4.2.1) and (4.2.2) is another possible abc.

$$\mathbf{n} \times \mathbf{P} + \alpha \frac{\mathrm{d}\mathbf{P}}{\mathrm{d}\mathbf{n}} = 0 \text{ with } \quad -1 \leq \alpha \leq 1 \,. \tag{4.2.3}$$

The abc was first studied by Pekar in [49] where the condition (4.2.1) was introduced. It turns out that experimentally observed spectra , e.g., of the exciton resonance , can be fitted with all above mentioned abc.

For a semiconductor with exciton-biexciton coupling confined inside, three branches of polariton waves exist. In order to deal with these three waves two abc are needed, which makes the analysis and computation very complicated and expansive. Fortunately, for finite but very small damping constants an asymptotic analysis shows that among the three modes only two dominate, and the third one can be safely eliminated without affecting the essential physics. Thus the complexity of the model and its computational cost, especially for the high dimensional case, can be greatly reduced.

For the analysis, a resonance case of $\omega = \omega_{\mathrm{ex}}$ in Eq. (4.1.2) is of interest and will be considered. We start with γ and β being zero, $a(\omega_{\mathrm{ex}}) < 0$, $b(\omega_{\mathrm{ex}}) < 0$ and $c(\omega_{\mathrm{ex}}) > 0$ can be seen for the medium, in addition $c(\omega_{\mathrm{ex}})$ is found to be an extremely small number. It can be shown via a perturbation analysis that $y^3 + a(\omega_{\mathrm{ex}})y^2 + b(\omega_{\mathrm{ex}})y + c(\omega_{\mathrm{ex}}) = 0$ has three real roots (let $y = k^2$); k_1^2, k_1^2 and k_3^2. Furthermore the relations $k_1^2 \cdot k_2^2 \cdot k_3^2 = -c(\omega_{\mathrm{ex}}) < 0$ and $k_1^2 + k_2^2 + k_3^2 = -a(\omega_{\mathrm{ex}}) > 0$ guarantee that one root is negative (e.g., k_2^2) and the other two are positive (k_1^2, k_3^2).

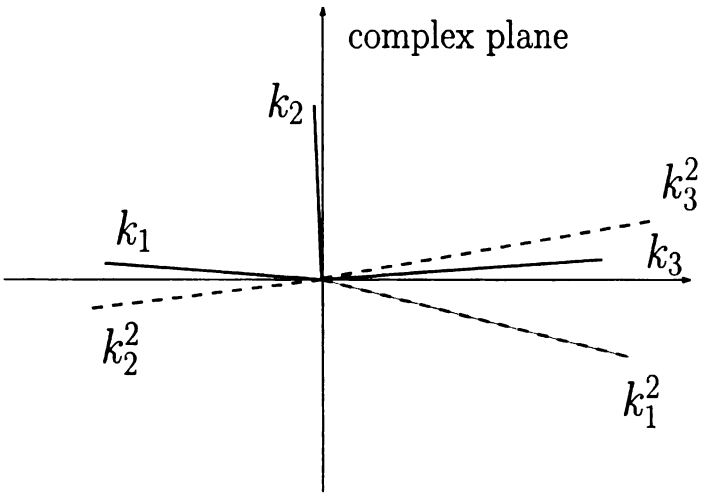

Figure 4.2: A sketch of the wavenumbers in the vicinity of a resonance $\omega = \omega_{\text{ex}}$ with very small damping constants is shown in the plot.

Next consider very small γ and β, then the coefficients a, b and c are going to be perturbed by very small complex numbers, so are the k_1^2, k_2^2 and k_3^2. Clearly, both k_1 and k_3 have very small imaginary parts, whereas the imaginary part of k_2 is relatively large, which are shown in Fig. 4.2. It should be noted that modes k_1 and k_3 will make considerable contribution to the light scattering. However, the contribution from mode k_2 is negligible. To calculate the reflection and transmission spectra of the slab, an additional boundary condition is still needed for these two waves, one possible argument is that the polarization induced by the exciton-biexciton transition must be zero at the interface.

To validate the approximation an optically excited CuCl nano slab is considered, the model Maxwell equations in the slab are

$$\frac{\mathrm{d}^2 E_i}{\mathrm{d}x^2} + k_i^2 E_i \ \ , i = 1, 3 \tag{4.2.4}$$

and the total field $E = E_1 + E_3$. Besides the additional boundary condition, the tangential components of the field and its derivative need to be continuous across the interface.

To illustrate the validation of our approximation, we present numerical computations of the reflection and transmission spectra of the slab. The thickness of the slab is 340 nm, and all other parameters are from CuCl semiconductor: $\varepsilon_{\mathrm{b}} = 5.59, \omega_{\mathrm{ex}} = 3.2022\mathrm{ev}, \omega_{\mathrm{bi}} = 6.372\mathrm{ev}, \hbar\omega_{\mathrm{pu}} = 3.1698\mathrm{ev}, M = 2.3m_0, \mu_{\mathrm{gx}}^2 = 2.513\mathrm{mev}, \mu_{\mathrm{xb}}^2 = 2 \times 10^{-3}\mathrm{mev}, \gamma = 1\mathrm{mev}, \beta = 0.015\mathrm{mev}$, where m_0 is the mass of an electron. If all the three polariton modes are considered, another boundary condition will be required. One physically plausible argument is that the polarization should vary smoothly across the interface, i.e., $\dfrac{\mathrm{d}P}{\mathrm{d}x} = 0$. The numerical simulations are plotted in Figures 4.3 (a) and (b), the peaks in the plots actually imply that exciton-biexciton transmission happens in the vicinity of $\omega = \omega_{\mathrm{ex}}$. In the resonance region, our approximation show good agreements with the three wave results. As we can see three polariton modes with same frequency but different wavenumbers are generated due to the exciton-biexciton transition in a thin semiconducting slab. We have shown that one of the modes can only penetrate a very small depth in the medium, hence it contributes little to the light scattering even if multiple reflections and transmissions are considered. Our criterion is to eliminate this mode and keep the other two. The approximate model is established via coupling Maxwell's equations with additional boundary conditions, which agrees well with the three waves model in the resonance

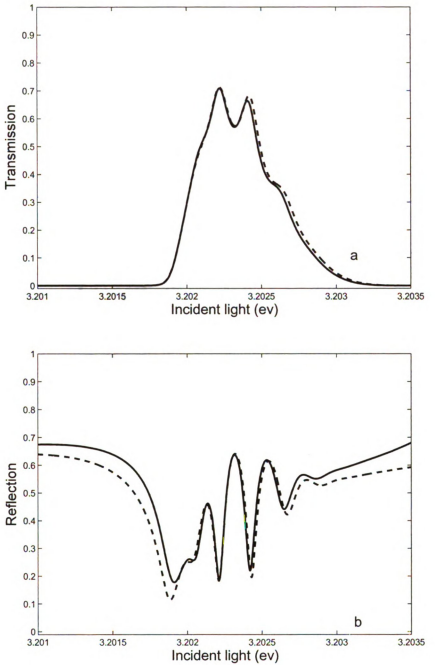

Figure 4.3: The transmission (a) and reflection (b) spectra of a CuCl slab of 340 nm thick. The solid curves are obtained from the two modes approximation, the dashed curves are resulted from the three modes computations.

region of interest.

In the following section we will establish the model partial differential equations and present several mathematical results concerning the existence and uniqueness of the solutions.

4.3 Model PDEs and theoretical results

Based on the criterion we proposed for exciton-biexciton coupling model, we are dealing with two waves for both exciton and biexciton cases. Mathematical models for the exciton and the coupling of exciton-biexciton are identical in terms of partial differential equations and additional boundary conditions. Eq. (3.1.10) for the electric field inside the medium is changed to

$$\nabla \times \nabla \times \mathbf{E} - (\frac{\omega}{c})^2 \varepsilon(k,\omega)\mathbf{E} = 0\,, \tag{4.3.1}$$

where $\mathbf{E} = \mathbf{E_a} + \mathbf{E_b}$, and $\mathbf{E_a}$, $\mathbf{E_b}$ satisfy following two equations

$$\nabla \times \nabla \times \mathbf{E}_a - k_a^2\mathbf{E} = 0\,, \nabla \times \nabla \times \mathbf{E}_b - k_b^2\mathbf{E} = 0\,. \tag{4.3.2}$$

On the boundary Γ, we impose additional boundary conditions as well as Maxwell's boundary conditions. Next we will specify the mathematical models for three special nanoscale structures, namely, slab, wire, and sphere. The well-posedness of the model partial differential equations is also presented.

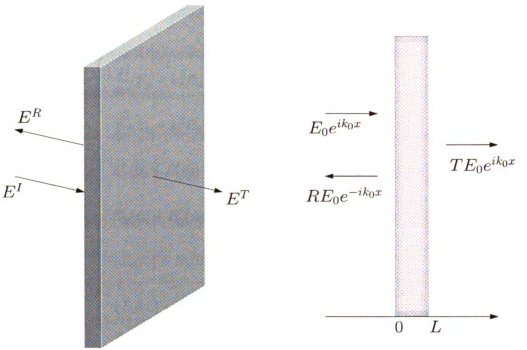

Figure 4.4: A nano slab. Left: the full view; Right: the one dimensional confinement view.

1. Nano slab. Consider the light scattering by a nano slab depicted in Fig. 4.4 for an incident plane wave. The exciton (biexciton) is confined in x axis due to the nanometer scale of the slab in that direction. As illustrated in Fig. 4.4, the incident field is $E_0e^{ik_0x}$, the reflected field is $RE_0e^{-ik_0x}$, and the transmitted field is $TE_0e^{ik_0x}$. To calculate the reflection and transmission coefficients R, T, we set up the equations inside the slab along with the boundary conditions. Here, $E = E_a + E_b$ is the total field inside the slab from two waves k_a, k_b.

Define the domain $\Omega = (0, L)$, we have derived the following boundary value

problem in [59]

$$\begin{cases} \frac{d^2}{dx^2}E_a + k_a^2 E_a = 0 \ \text{ in } \Omega\,, \\ \frac{d^2}{dx^2}E_b + k_b^2 E_b = 0 \ \text{ in } \Omega\,, \\ E_a'(0) + E_b'(0) = -ik_0(E_a(0) + E_b(0)) + 2ik_0 E_0\,, \\ E_a'(L) + E_b'(L) = ik_0(E_a(L) + E_b(L))\,, \\ \chi E_a(0) + E_b(0) = 0\,, \\ \chi E_a(L) + E_b(L) = 0\,, \end{cases} \tag{4.3.3}$$

where $\chi = \dfrac{\chi(k_a)}{\chi(k_b)}$. By introducing $u(x) = \chi E_a(x) + E_b(x)$, $v(x) = E_a(x) + E_b(x)$, the system (4.3.3) may be rewritten as

$$\begin{cases} \frac{d^2}{dx^2}u + \frac{\chi k_b^2 - k_a^2}{\chi - 1}u + \frac{\chi(k_a^2 - k_b^2)}{\chi - 1}v = 0 \ \text{ in } \Omega\,, \\ \frac{d^2}{dx^2}v + \frac{\chi k_a^2 - k_b^2}{\chi - 1}v + \frac{k_b^2 - k_a^2}{\chi - 1}u = 0 \ \text{ in } \Omega\,, \\ v'(0) = -ik_0 v(0) + 2ik_0 E_0\,, \\ v'(L) = ik_0 v(L)\,, \\ u(0) = u(L) = 0\,. \end{cases} \tag{4.3.4}$$

Our well-posedness result of the model problem is stated as follows

Theorem 4.3.1. *For all but a possibly discrete set of the frequencies ω, the model problem (4.3.4) attains a unique solution $(u, v) \in H_0^1(\Omega) \times H^1(\Omega)$.*

Proof. Multiplying the first and second equations in (4.3.4) by the test functions $\xi \in H_0^1(\Omega)$ and $\eta \in H^1(\Omega)$, we get after some simple integration by parts and making use of boundary conditions

$$\int_\Omega \nabla U \cdot \nabla \overline{V} + \int_\Omega AU \cdot \overline{V} + ik_0 \int_{\partial\Omega} BU \cdot \overline{V} = 2ik_0 BV \,, \tag{4.3.5}$$

where $U = [u, v]$, $V = [\xi, \eta]$, $\nabla U = [u', v']$, the overline denotes the complex conjugation, and

$$A = A(\omega) = -\begin{pmatrix} \frac{\chi k_b^2 - k_a^2}{\chi - 1} & \frac{\chi(k_a^2 - k_b^2)}{\chi - 1} \\ \frac{k_b^2 - k_a^2}{\chi - 1} & \frac{\chi k_a^2 - k_b^2}{\chi - 1} \end{pmatrix}, \qquad B = \begin{pmatrix} 0 & 0 \\ 0 & -1 \end{pmatrix}. \tag{4.3.6}$$

Defining $W(\Omega) = H_0^1(\Omega) \times H^1(\Omega)$, we introduce the bilinear form $a : W(\Omega) \times W(\Omega) \to \mathbb{C}$,

$$a(U, V) = (\nabla U, \nabla V) + ik_0 (BU, V)_{\partial\Omega} + (AU, V) \,, \tag{4.3.7}$$

and the linear functional on $W(\Omega)$,

$$b(V) = 2ik_0 BV \,.$$

Next, we decompose a into $a_1 + a_2$, where

$$a_1(U, V) = (\nabla U, \nabla V) + ik_0 (BU, V)_{\partial\Omega} \,, a_2(U, V) = (AU, V) \,.$$

Using the fact that k_0 is positive and Poicaré's inequality [19], we see that

$$\begin{aligned} |a_1(U,U)| &\geq c\Big(\int_\Omega |u'|^2 + \int_\Omega |v'|^2 + k_0|v(0)|^2\Big) \\ &\geq c||u||^2_{H^1(\Omega)} + c(L,k_0)||v||^2_{H^1(\Omega)} \\ &\geq \gamma(L,k_0)||U||^2_{W(\Omega)} , \end{aligned}$$

where $||U||^2_{W(\Omega)} = ||u||^2_{H^1(\Omega)} + ||v||^2_{H^1(\Omega)}$.

Then the coercivity of a_1 is obtained, thus the Lax-Milgram lemma implies that the operator $\mathcal{A}_1$ defined by $\langle \mathcal{A}_1 U, V\rangle = a_1(U,V)$ has a bounded inverse. Note that the operator $\mathcal{A}_2$ defined by $\langle \mathcal{A}_2 U, V\rangle = a_2(U,V)$ is compact. To emphasize that both $\mathcal{A}_1$ and $\mathcal{A}_2$ depend on the frequency ω, we write $\mathcal{A}_1(\omega)$, $\mathcal{A}_2(\omega)$.

Holding ω_1 fixed, consider the operator $\mathcal{A}(\omega_1,\omega) = \mathcal{A}_1(\omega_1) + \mathcal{A}_2(\omega)$. Since $\mathcal{A}_1$ is bounded invertible and $\mathcal{A}_2$ is compact, we see that $\mathcal{A}(\omega_1,\omega)^{-1}$ exists by Fredholm theory for all $\omega \notin \mathcal{E}(\omega_1)$, where $\mathcal{E}(\omega_1)$ is some discrete set. It is clear that

$$||\mathcal{A}_1(\omega) - \mathcal{A}_1(\omega_1)|| \to 0 \ \text{ as } \omega \to \omega_1 .$$

Thus since $||\mathcal{A}(\omega,\omega) - \mathcal{A}(\omega_1,\omega)|| = ||\mathcal{A}_1(\omega) - \mathcal{A}_1(\omega_1)||$ is small for $|\omega - \omega_1|$ sufficiently small, it follows from the stability of bounded invertibility (see, e,g., [31]) that $\mathcal{A}(\omega,\omega)^{-1}$ exists and is bounded for $|\omega - \omega_1|$ sufficiently small, $\omega \notin \mathcal{E}(\omega_1)$. Since $\omega_1 > 0$ can be an arbitrary real number, we have shown that $\mathcal{A}(\omega,\omega)^{-1}$ exists for all but a discrete set of points. □

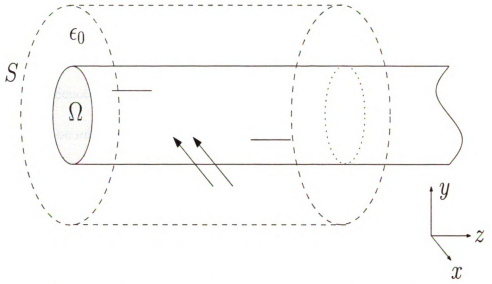

Figure 4.5: A nano wire structure confines the exciton and biexciton in x, y directions but allows them to move along z-axis.

2. Nano wire. An infinite cylindrical nano wire with cross-section Ω is depicted in Fig. 4.5. For normally incident field $(0, 0, E^i(x, y))$, there exist two fields E_a, E_b inside the wire with wavenumbers k_a, k_b, the governing equations are the Helomholtz equations,

$$(\nabla_T^2 + k_a^2)E_a = 0 \, , (\nabla_T^2 + k_b^2)E_b = 0 \, ,$$

where $\nabla_T^2 = \partial_x^2 + \partial_y^2$, and the total field inside is $E = E_a + E_b$. The total field outside the of the wire consists of the incident field E^i and the scattered field E^s. The scattered field is outgoing and this is imposed by requiring the scattered field to satisfy the following Sommerfeld radiation condition:

$$\lim_{\rho \to \infty} \sqrt{\rho}(\frac{\partial}{\partial \rho} E^s + ik_0 E^s) = 0 \, ,$$

where $\rho = \sqrt{x^2 + y^2}$. In practice, it is convenient to reduce the problem to a bounded

domain by introducing an artificial boundary. Assume that $R > 0$ is a constant such that Ω is contained in the disk $D = \{x \in \mathbb{R}^2 : |x^2+y^2| < R^2\}$. Let S be the boundary of the disk, denote by ν the outward unit normal to S. A suitable boundary conditions then has to be imposed on S. For instance, we use the first order absorbing boundary condition [18] as

$$\frac{\partial}{\partial \nu} E^s + ik_0 E^s = 0 \text{ on } S\,. \tag{4.3.8}$$

Then we can derive the following system

$$\begin{cases} \nabla_T^2 u + a_1 u + b_1 v = 0 \ \text{ in } \Omega\,, \\ \nabla_T^2 v + a_2 v + b_2 u = 0 \ \text{ in } \Omega\,, \\ \nabla_T^2 v + k_0^2 v = 0 \ \text{ in } D/\Omega\,, \\ u = 0 \ \text{ on } \partial\Omega\,, \\ \frac{\partial}{\partial \nu} v + ik_0 v = \frac{\partial}{\partial \nu} E^i + ik_0 E^i \ \text{ on } S\,, \end{cases} \tag{4.3.9}$$

where $u(x,y) = \chi E_a + E_b$, $v(x,y) = E_a + E_b$, $a_1 = \dfrac{\chi k_b^2 - k_a^2}{\chi - 1}$, $b_1 = \dfrac{\chi(k_a^2 - k_b^2)}{\chi - 1}$, $a_2 = \dfrac{\chi k_a^2 - k_b^2}{\chi - 1}$, and $b_2 = \dfrac{k_b^2 - k_a^2}{\chi - 1}$.

Notice that the field $u(x,y)$ is compactly supported by domain Ω, we extend u by zero outside of Ω. To state our variational problem, we first introduce the Sobolev space:

$$H_t^1(D) = \{w \in H^1(D) : w \equiv 0 \text{ for } (x,y) \in \text{closure}(D)/\Omega\}\,,$$

Then we obtain the following weak form

$$\int_\Omega \nabla_T U \cdot \nabla_T \overline{V} - \int_{D/\Omega} B\nabla_T U \cdot \nabla_T \overline{V} + k_0^2 \int_{D/\Omega} BU \cdot \overline{V} + ik_0 \int_S BU \cdot \overline{V} \,,$$
$$+ \int_\Omega AU \cdot \overline{V} = \int_S (ik_0 E^i + \frac{\partial}{\partial \nu} E^i)\eta \,,$$

where the same notations as in the slab case are used, and A, B are defined in (4.3.6).

Define

$$\begin{aligned} a(U,V) &= (\nabla_T U, \nabla_T V)_\Omega - (B\nabla_T U, \nabla_T V)_{D/\Omega} + k_0^2 (BU, V)_{D/\Omega} \,, \\ &\quad + ik_0 (BU, V)_S + (AU, V)_\Omega \,. \end{aligned}$$

We write $a(U,V) = a_1(U,V) + a_2(U,V)$ with

$$\begin{aligned} a_1(U,V) &= (\nabla_T U, \nabla_T V)_\Omega - (B\nabla_T U, \nabla_T V)_{D/\Omega} + ik_0 (BU, V)_S \,, \\ a_2(U,V) &= k_0^2 (BU, V)_{D/\Omega} + (AU, V)_\Omega \,. \end{aligned}$$

By writing (x,y) into the polar coordinates system (r,θ) with $x = r\cos\theta, y = r\sin\theta$, we get

$$\begin{aligned} v^2(r,\theta) r &= Rv^2(R,\theta) - \int_r^R (\rho v^2(\rho,\theta))\rho d\rho \\ &= Rv^2(R,\theta) - \int_r^R v^2(\rho,\theta) d\rho - 2\int_r^R v v_\rho(\rho,\theta) d\rho \\ &\leq Rv^2(R,\theta) - 2\int_r^R \rho v \nabla v \cdot \frac{(x,y)}{\rho} d\rho \,, \end{aligned}$$

$$\int_0^R \int_0^{2\pi} |v^2(r,\theta)| r dr d\theta \leq c_1 \int_S |v|^2 + c_2 \int_D |v||\nabla v| ,$$
$$\int_D |v|^2 \leq c\Big(\int_D |\nabla v|^2 + k_0 \int_S |v|^2\Big) .$$

The coercivity of a_1 can be obtained by

$$\begin{aligned} |a_1(U,U)| &\geq c\Big(\int_\Omega |\nabla u|^2 + \int_D |\nabla v|^2 + k_0 \int_S |v|^2\Big) \\ &\geq c||u||^2_{H^1(D)} + c(R,\omega)||v||^2_{H^1(D)} \\ &\geq \gamma ||U||^2_{W(D)}, \end{aligned}$$

where $W(D) = H^1_t(D) \times H^1(D)$, $||U||^2_{W(D)} = ||u||^2_{H^1(D)} + ||v||^2_{H^1(D)}$, and γ depends on the size of D and ω.

Then by applying the similar argument as in the slab case, we can prove that the operator $\mathcal{A}$ defined by $\langle \mathcal{A}U, V\rangle = a(U,V)$ has a bounded inverse for all but a discrete set of points. Hence the model system (4.3.9) obtains a unique solution $(u,v) \in H^1_t(D) \times H^1(D)$ for all but a countable set of the frequencies ω.

A parallel waveguide case has recently been considered in [59], where the exciton is confined in a nano square imbedded between the plates of the waveguide. The well-posedness of that model follows immediately from a similar proof as the above.

3. Nano sphere. Suppose a semiconducting nano sphere with radius R is exposed to a plane wave $(\mathbf{E^i}, \mathbf{H^i})$, the Maxwell equations in three dimensions are

$$\nabla \times \mathbf{E} = i\frac{\omega}{c}\mathbf{H} , \nabla \times \mathbf{H} = -i\varepsilon\frac{\omega}{c}\mathbf{E} , \tag{4.3.10}$$

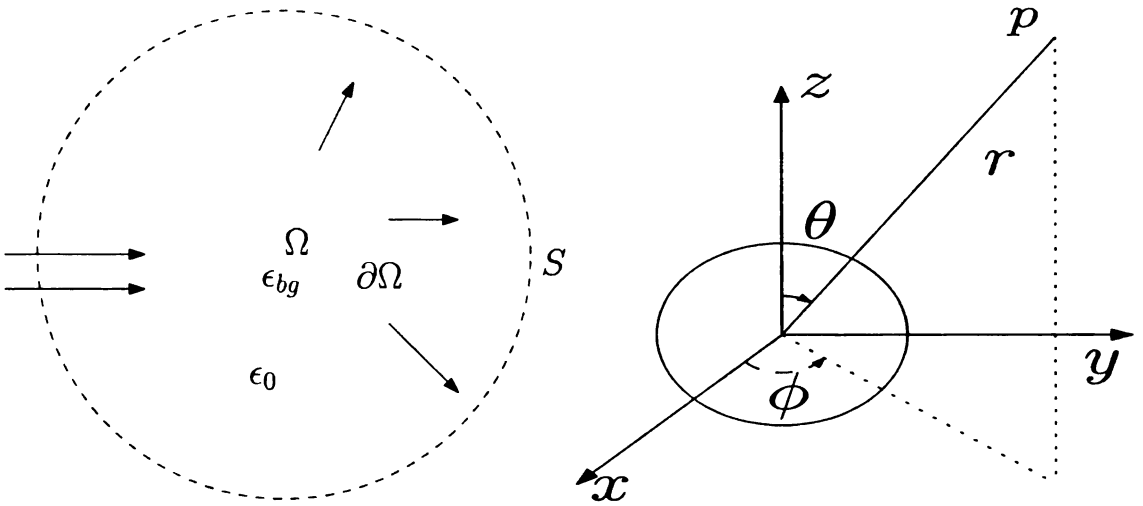

Figure 4.6: Left: A nano sphere can give the confinement in all three directions. Right: Spherical polar coordinate system centered at the sphere.

where

$$\varepsilon = \begin{cases} \varepsilon_0 & \text{outside} \\ \varepsilon(k,\omega) & \text{inside} \end{cases}$$

The divergence of (4.3.10) gives $\nabla \cdot \mathbf{E} = \nabla \cdot \mathbf{H} = 0$ because the medium is homogeneous. Then the governing equations become

$$\nabla^2\mathbf{E} + k_a^2\mathbf{E} = 0\,, \nabla^2\mathbf{H} + k_a^2\mathbf{H} = 0\,,$$

$$\nabla^2\mathbf{E} + k_b^2\mathbf{E} = 0\,, \nabla^2\mathbf{H} + k_b^2\mathbf{H} = 0\,.$$

It is more appropriate in this case to present problem in spherical polar coordinates, r, θ, ϕ in Fig. 4.6 defined by

$$x = r\sin\theta\cos\phi\,, y = r\sin\theta\sin\phi\,, z = r\cos\theta\,.$$

Consider an x-polarized incident plane wave, written in spherical coordinates $\mathbf{E}^i = E_0 e^{ik_0 z}\mathbf{x}$, where

$$\mathbf{x} = \sin\theta\cos\phi\mathbf{e}_r + \cos\theta\cos\phi\mathbf{e}_\theta - \sin\phi\mathbf{e}_\phi \ .$$

There are three kinds of fields in our system: the incident field $(\mathbf{E}^i, \mathbf{H}^i)$, the scattered field $(\mathbf{E}^s, \mathbf{H}^s)$, and the field $(\mathbf{E}^w, \mathbf{H}^w)$ within the sphere. Following Lorenz-Mie scattering theory, we expand all those fields in terms of vector spherical harmonics,

$$\mathbf{E}^i = \sum_{n=1}^{\infty} E_n(\mathbf{M}_{o1n}^{(1)} - i\mathbf{N}_{e1n}^{(1)}) \ , \mathbf{H}_i = -\sqrt{\epsilon_0}\sum_{n=1}^{\infty} E_n(\mathbf{M}_{e1n}^{(1)} + i\mathbf{N}_{o1n}^{(1)}) \ ,$$

$$\mathbf{E}^s = \sum_{n=1}^{\infty} E_n(a_n^s\mathbf{M}_{o1n}^{(2)} - ib_n^s\mathbf{N}_{e1n}^{(2)}) \ , \mathbf{H}^s = -\sqrt{\epsilon_0}\sum_{n=1}^{\infty} E_n(b_n^s\mathbf{M}_{e1n}^{(2)} + ia_n^s\mathbf{N}_{o1n}^{(2)}) \ ,$$

and

$$\mathbf{E}_j^w = \sum_{n=1}^{\infty} E_n(a_n^j\mathbf{M}_{o1n}^{(1)} - ib_n^j\mathbf{N}_{e1n}^{(1)}) \ , \mathbf{H}_j^w = -\sqrt{\epsilon_j}\sum_{n=1}^{\infty} E_n(b_n^j\mathbf{M}_{o1n}^{(1)} - ia_n^j\mathbf{N}_{e1n}^{(1)}) \ ,$$

where $j = 1, 2$ and $\varepsilon_1 = \varepsilon(k_a, \omega)$, $\varepsilon_2 = \varepsilon(k_b, \omega)$, $E_n = i^n(2n+1)/n(n+1)$, and we append the superscript (1) and (2) to vector spherical harmonics for which the radial dependence of the generating functions are specified by Bessel function of first kind $j_n(r)$ and Hankel function of first kind $h_n(r) = j_n(r) + iy_n(r)$, where

$$\mathbf{M}_{emn} = \frac{-m}{\sin\theta}\sin m\phi P_n^m(\cos\theta)z_n(\rho)\mathbf{e}_\theta - \cos m\phi(P_n^m(\cos\theta))_\theta z_n(\rho)\mathbf{e}_\phi \ ,$$

$$
\begin{aligned}
\mathbf{M}_{omn} &= \frac{m}{\sin\theta}\cos m\phi P_n^m(\cos\theta)z_n(\rho)\mathbf{e}_\theta - \sin m\phi(P_n^m(\cos\theta))_\theta z_n(\rho)\mathbf{e}_\phi\,, \\
\mathbf{N}_{emn} &= \frac{z_n(\rho)}{\rho}\cos m\phi n(n+1)P_n^m(\cos\theta)\mathbf{e}_r + \cos m\phi(P_n^m(\cos\theta))_\theta\frac{1}{\rho}(\rho z_n(\rho))_\rho\mathbf{e}_\theta \\
&\quad -m\sin m\phi\frac{P_n^m(\cos\theta)}{\sin\theta}\frac{1}{\rho}(\rho z_n(\rho))_\rho\mathbf{e}_\phi\,, \\
\mathbf{N}_{omn} &= \frac{z_n(\rho)}{\rho}\sin m\phi n(n+1)P_n^m(\cos\theta)\mathbf{e}_r + \sin m\phi(P_n^m(\cos\theta))_\theta\frac{1}{\rho}(\rho z_n(\rho))_\rho\mathbf{e}_\theta \\
&\quad +m\cos m\phi\frac{P_n^m(\cos\theta)}{\sin\theta}\frac{1}{\rho}(\rho z_n(\rho))_\rho\mathbf{e}_\phi
\end{aligned}
$$

with z_n is any of the four spherical Bessel functions j_n, y_n, $h_n^{(1)} = j_n(r) + iy_n(r)$ and $h_n^{(2)} = j_n(r) - iy_n(r)$. The derivation of $\mathbf{M}_{emn}$, $\mathbf{M}_{omn}$, $\mathbf{N}_{emn}$, and $\mathbf{N}_{omn}$ is a standard topic in Mie theory and will not be repeated here, see for instance [8, 62].

The unknown coefficients a_n^s, b_n^s, a_n^j, b_n^j are determined by the boundary conditions at $r = R$,

$$
\begin{aligned}
E_\theta^i + E_\theta^s &= E_{1\theta}^w + E_{2\theta}^w\,, \\
E_\phi^i + E_\phi^s &= E_{1\phi}^w + E_{2\phi}^w\,, \\
H_\theta^i + H_\theta^s &= H_{1\theta}^w + H_{2\theta}^w\,, \\
H_\phi^i + H^s\phi &= H_{1\phi}^w + H_{2\phi}^w\,, \\
\chi(k_a,\omega)E_{1\theta}^w + \chi(k_b,\omega)E_{2\theta}^w &= 0\,, \\
\chi(k_a,\omega)E_{1\phi}^w + \chi(k_b,\omega)E_{2\phi}^w &= 0\,.
\end{aligned}
$$

With these boundary conditions, we obtain:

$$a_n^s = \frac{jnR_0(\chi r)(k_aRjn(R_a))' - (k_0Rjn R_0)'(\sqrt{\epsilon_a}jn(R_a) - \chi\sqrt{\epsilon_b}jn(R_b)\frac{(k_aRjn(R_a))'}{(k_bRjn(R_b))})}{hnR_0(\chi r)(k_aRjn(R_a))' - (k_0Rhn R_0)'(\sqrt{\epsilon_a}jn(R_a) - \chi\sqrt{\epsilon_b}jn(R_b)\frac{(k_aRjn(R_a))'}{(k_bRjn(R_b))})},$$

$$b_n^s = \frac{jnR_0(\sqrt{\epsilon_a}(k_aRjn(R_a))' - \chi\sqrt{\epsilon_b}(k_bRjn(R_b))'\frac{jn(R_a)}{jn(R_b)}) - (k_0Rjn R_0)'jn(R_a)(\chi r)}{hnR_0(\sqrt{\epsilon_a}(k_aRjn(R_a))' - \chi\sqrt{\epsilon_b}(k_bRjn(R_b))'\frac{jn(R_a)}{jn(R_b)}) - (k_0Rhn R_0)'jn(R_a)(\chi r)},$$

where the derivatives of these functions are denoted by primes, $\chi r = 1-\chi$, $R_0 = k_0R$, $R_a = k_aR$ and $R_b = k_bR$. The scattering cross section is given by the standard Mie formula

$$Q_{sca} = \frac{2}{{R_0}^2}\sum_{n=1}^{\infty}(2n+1)(\text{abs}(a_n^s)^2 + \text{abs}(b_n^s)) .$$

Chapter 5

NUMERICAL EXPERIMENTS

In this part the dielectric constant model will be applied to CuCl nanocrystals of different dimensions. There are several reasons why CuCl is a rather well studied model materials [30]. CuCl is a typical material for exciton/biexciton confinements [60], and its excitons have a relative small Bohr radius (about 0.7nm), and a large binding energy (about 2ev). Very recently, CuCl has attracted research interests once more, due to the ability of the excitons in CuCl to form biexcitons, which are potential candidates to undergo a Bose-Einstein condensation. In fact, evidence has been obtained in [25, 42] that excitonic excitations in semiconductors like CuCl exhibit features expected in a weakly Bose gas. In the following we will show the optical response results for excitons and biexcitons confined in one, two and three dimensional CuCl nanocrystals. The parameters used in the numerical simulations are $\epsilon_b = 5.59, \epsilon_0 = 1.0, \hbar\omega_0 = 3.2022\text{ev}, M = 2.3m_0, \mu_{gx}^2 = 2.513\text{mev}, \gamma = 1\text{mev}, \hbar\omega_p = 3.168\text{ev}, \hbar\omega_b = 6.372\text{ev}, M_b = 2M, \beta = 5 \times 10^{-7}\text{ev}^2, \gamma_b = 0.015\text{mev}$, where m_0 is

the mass of an electron.

5.1 CuCl nano slab

The optical responses by exciton/exciton-biexciton coupling in a CuCl slab are calculated. The reflection and transmission spectra are plotted. For the numerical simulations a plane wave with wavelength λ in the range of [380, 400] nm are used. First the exciton effects are considered, hence the dielectric constant (3.2.7) is used. Fig. 5.1 shows the spectra of the transmitted and reflected lights by CuCl slab of different sizes. The resonant structures showed in the figures are due to the exciton mode, interfering with the size resonance of the slab. The excitons in a semiconductor slab is a well studied case for various thicknesses including a semi-infinite limit [12, 15, 28]. In theory, if all the multiple reflection effects are neglected, two kinds of oscillatory effects should be observed. One is periodic modulation of the transmission at fixed energy as a function of the thickness. The other is a periodic modulation of the transmission at fixed thickness as a function of the energy. Both these two effects are clearly verified in our numerical experiments. Compared with the normal incidence reflection experiments in CdS [15], the experimental line shape, especially the resonance peaks are well produced. Also from Figure 5.1, the peaks of spectral transmission and reflection clearly indicate enhanced optical absorptions, and those peaks move to the right as the CuCl slab thickness decreases, which is the well known **blue shift** phenomenon.

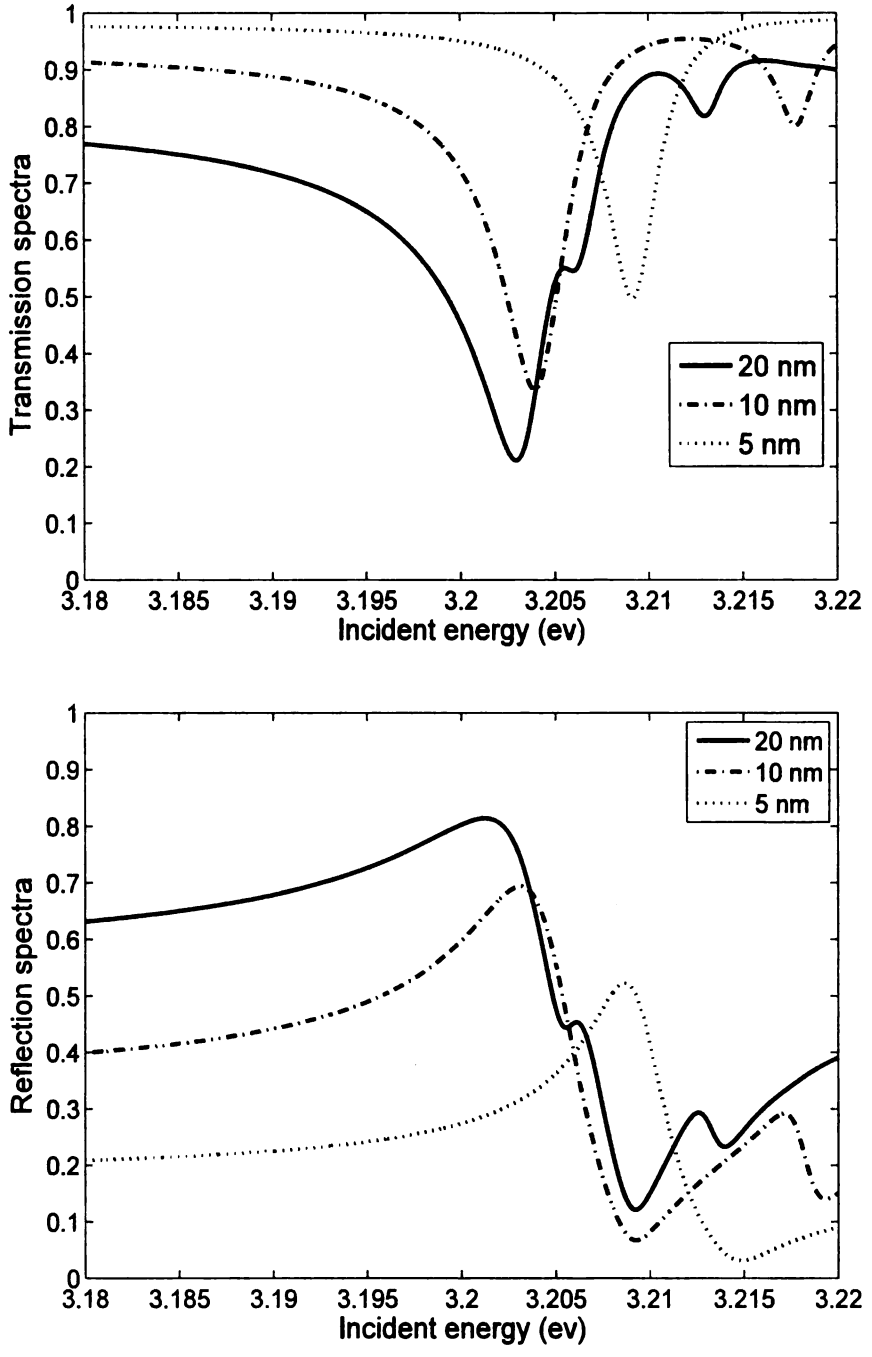

Figure 5.1: Size dependence of spectral transmission and reflection of the CuCl slab. The horizontal axis is the incident energy (ev). Top: transmission spectrum. Bottom: reflection spectrum.

Then for the exciton-biexciton coupling in the CuCl slab, numerical results are obtained based on the two dominant modes approximation. If we view the two boundary points of the slab ($x = 0\ , L$) as two dipole emitters, then a separation Δr between the dipoles

$$\Delta r \approx \frac{2\lambda}{n}$$

defines the axial resolution (or the depth resolution) of the system. n is the refractive index of the medium.

The axial resolution sets a limit to the ability of an optical system in the optical sectioning and three dimensional imaging. In order to achieve a better image, the axial resolution has to be improved. Many approaches have been proposed to enhance the axial resolution in nano-optics, for example, one important technique is to use the nonlinear excitation. we refer the reader to the book [46] for more details and references.

When the thickness L of the CuCl slab is bigger than the axial resolution $\Delta r \approx$ 340nm, we receive almost no contribution from the left dipole ($x = 0$) in the transmission spectrum, or we can get a stop band within which the light is nearly completely reflected in Figure 5.3. The second plot in Figure 5.2 indicates a nonlinear response of the medium, the exciton-biexciton coupling opens a narrow window in the transmission band, which confirms the enhancement of the axial resolution which benefits from the nonlinear excitation.

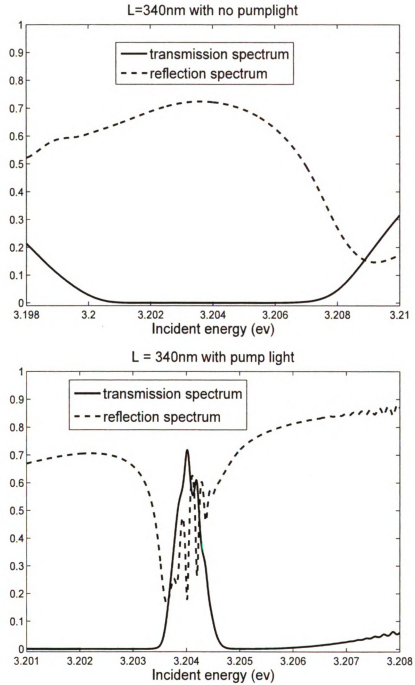

Figure 5.2: Tom: A stop band for the excitonic transmission without pumping light. Bottom: Due to the exciton-biexciton coupling in a pumping light $\hbar\omega_p = 3.168\text{ev}, \beta = 2 \times 6\text{ev}^2$, the nonlinear enhancement happens at $\hbar\omega = 3.204\text{ev}$ which is the binding energy to form a biexciton.

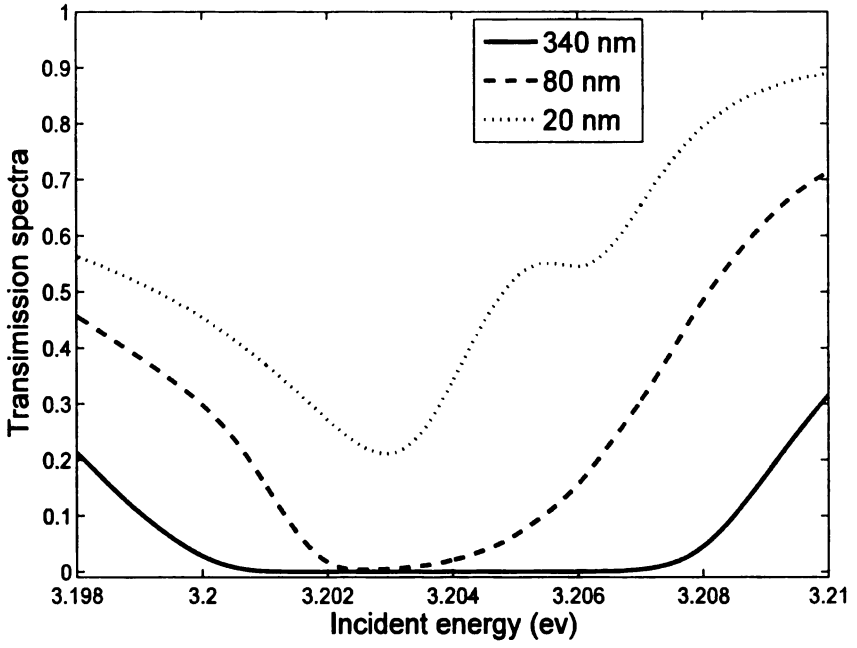

Figure 5.3: A stop band in transmission spectra is observed for $L = 340$nm. More light is transmitted through the slab as the thicknesses decrease.

5.2 Quantum dots

From the simulation results in the three dimensional case, we plot the scattering cross sections in Fig. 5.4. Clearly blue shift phenomena are observed when the radii of the sphere decrease. The blue shift is the shortening of a transmitted signal's wavelength, and an increase in its frequency. Furthermore, in the exciton case the peaks of the cross sections are around $\hbar\omega = 3.2022$ev, in fact this is the exact amount of energy required to form an exciton. For the biexciton case, a pump light is applied with energy 3.168ev in addition to a probe light with the energy varying. To supply enough energy to bind two excitons forming a biexction, we need $6.372\text{ev} - 3.168\text{ev} = 3.204$ev, and this amount of energy is provided from the probe light. Therefore, the peaks in the biexciton case happen at around $\hbar\omega = 3.204$ev.

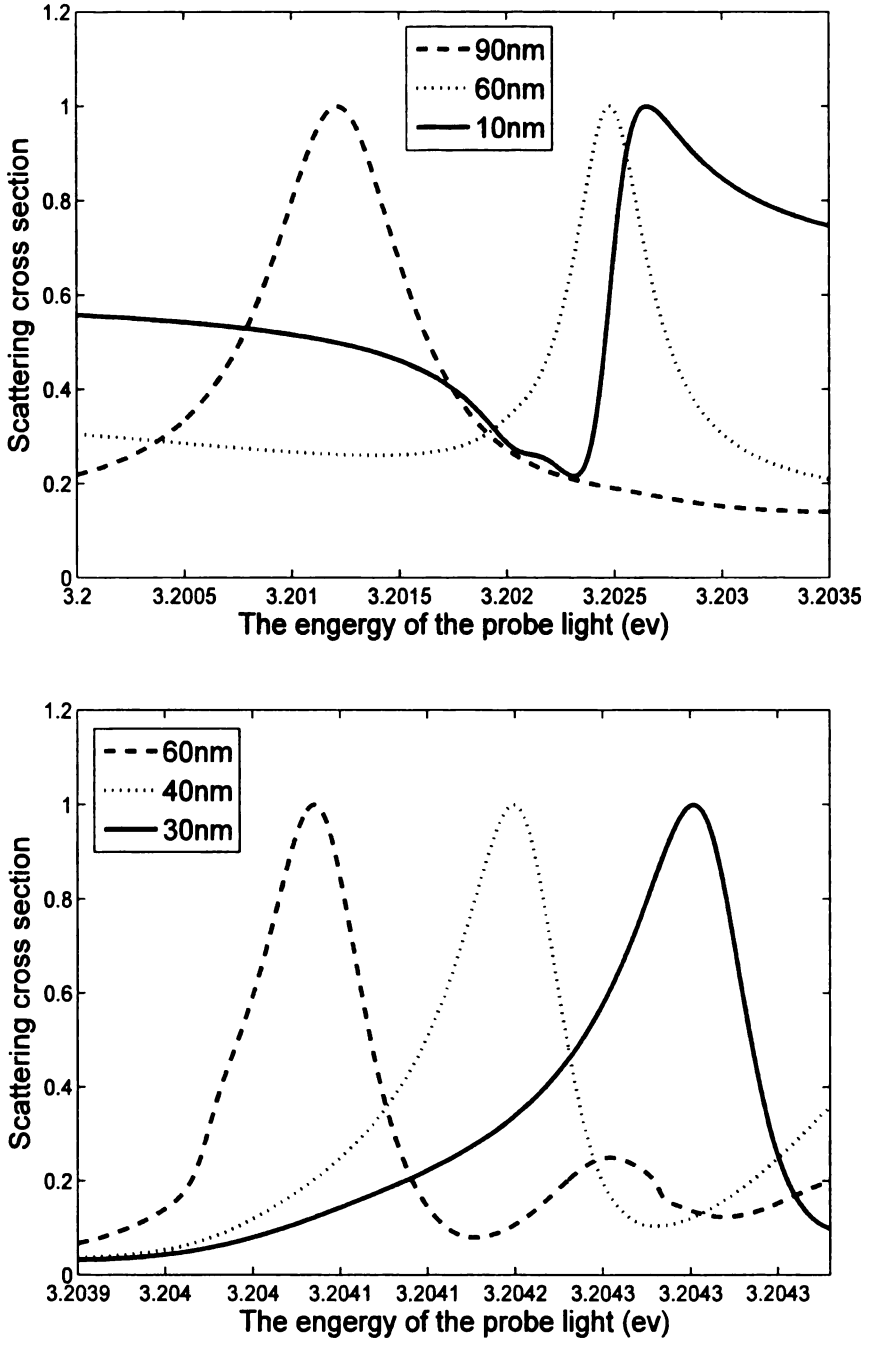

Figure 5.4: Top: Scattering cross sections of the exciton response. Bottom: Scattering cross sections of the exciton-biexciton coupling response. The cross sections are normalized so that their maxima will be unity.

Based on the results presented above, we can conclude that, due to the excitation of exciton polariton, the optical properties of a nano sphere (quantum dot) vary strongly around the ground-state exciton resonance frequency ω_0. For example, if we consider a single CuCl quantum dot with a radius of 60 nm, the corresponding resonant wavelength is about 380 nm. An electromagnetic wave with a wavelength of about 380 nm (in optical regime) will then be significantly manipulated by such a QD whose thickness is as small as 60 nm. These facts have a bearing on the use of exciton polaritons for beating the diffraction limit of light.

Chapter 6

CONCLUSIONS AND FUTURE WORKS

This thesis has presented a modeling and computational study in optical responses of nanostructured media. Particular interests have been placed on semiconducting materials due to their extensive applications in optical sciences. Under the condition of weak confinement a nonlocal dispersive dielectric constant (depends on k and ω) has been derived via coupling Maxwell's equations and Schrödinger equation, a semiclassical model hence is established by incorporating this new dielectric constant to the Maxwell's equation. The wellposedness of the model partial differential equations is studied for the first time, and the exciton and biexction effects on the nanometer scale have been extensively investigated in the thesis. It has been shown that the blue shift phenomena and nonlinear electromagnetically induced transparency effect can be well predicted from the semiclassical model. In addition to nonlocal effects

of the optical response, the finite size effects on the optical properties are also investigated in terms of eigenfrequencies and oscillator strengths of the excitations in nanocrystals. Although semiconducting nanostructures have been the primary focus of the thesis, the semiclassical framework of the present approach should be able to generalized to other materials, for example, metallic nanostructures which have been recently gaining extensive research efforts. While physicists and engineers have designed and fabricated many novel metallic nanostructures being used in laboratories, little is known about the rigorous modeling and efficient computation of the optical responses. A future work is to investigate the optical interactions with metallic nanostructures. The study of optical phenomena related to electromagnetic response of metals is termed plasmonics or nanoplasmonics which has been growing really rapid over the past few years. It mostly deals with the control of optical radiation on the nanometer scales. Many innovative concepts and applications have been developed in recent years and the following section will introduce a few examples. Most importantly some open and challenging problems will be discussed.

6.1 Plasmons in metallic nanostructures

The interaction of metals with electromagnetic radiation is largely dictated by the free conduction electrons in the metal. Collective oscillations of the conduction electrons, termed plasmons, strongly influence the optical properties of metal nanostructures and are of great interest for future photonic devices. Many (but not all) properties of

real metals, including their optical properties as described by the frequency dependent dielectric function $\varepsilon(\omega)$, are surprisingly well predicted from the so called Drude-Sommerfeld model [46]. The resulting equation is:

$$\varepsilon(\omega) = \varepsilon_\infty - \frac{\omega_p^2}{\omega(\omega + i\gamma_0)}$$

with ω_p the so-called plasma frequency and γ_0 the electron relaxation rate. ε_∞ includes the contribution of the bound electrons to the polarizability and should have the value of 1 if only the conduction band electrons contribute to the dielectric function. The plasma frequency is given by $\omega_p = \sqrt{Ne^2/\varepsilon_0 m^*}$ with N and m^* being the density and effective mass of the conduction electrons, respectively. The electron relaxation time can be calculated from the DC conductivity σ by $\tau = \sigma m^*/Ne^2$. Although the Drude-Sommerfeld theory give quite accurate predictions for bulk metals, some quantum effects such as surface scattering and quantum confinement effects become more important in nanosized metallic particles. For small particles with high surface to volume ratio surface scattering leads to additional collisions of the conduction electrons with a rate τ^{-1}, proportional to the Fermi-velocity v_F (about 1.4 nm/fs in Au and Ag). The additional damping surface is given empirically by

$$\gamma_s^{-1} = Av_F/r\ ,$$

where r is the particle radius and an empirical parameter A describing the loss of coherence by the scattering event. A is found to be dependent on surface chemistry, i.e. the type and strength of chemical interaction of adsorbates to the surface. Typical values in silver are between 0.1 and 0.7. Confinement of free electrons leads to notable quantum confinement effects as the dimension of the particle reaches the level of the Fermi wavelength of the free electron (about 0.7 nm), discrete, quantum-confined electronic transitions appears [65]. It should be emphasized that the understanding of quantum confinement is made possible only when a full quantum mechanical treatment is invoked. However, little work has been done in this regard and it deserves more research efforts.

The eigenmodes of collective oscillations of the quasi-free electrons in metals are called plasmons. The existence of plasmons is a characteristic of the interaction of metallic nanostructures with light. Similar behavior cannot be simply reproduced in other spectral ranges using the scale invariance of Maxwell's equations since the material parameters change considerably with frequency. Because electrons carry a charge, these oscillations are inherently associated with an electromagnetic field. Therefore a theoretical description has to include this interplay of charges and fields. The boundary conditions for electromagnetic fields lead to different conditions for the occurrence of plasmons for the cases of planar metal-dielectric interfaces and metal particles. The surface charge density of oscillation associated with surface plasmons at the interface between a metal and dielectric can give rise to strongly

enhanced optical near-fields **which** is confined near the metal surface. Similarly, if the electron gas is confined **in** two dimensions or three dimensions, as in the cases of a nano wire and nanoparticle, the overall displacement of the electrons with respect to the positively charged lattice leads to a restoring force, which in turn gives rise to specific particle-plasmon resonance. For the understanding of surface plasmons, it is very useful to study the results of simple electrodynamical theory applied to an ideal model interface. Obviously this approach neglects many real effects due to the exact surface properties, screening effects, quantum mechanical corrections, etc.. However, the main features of surface plasmons can be understood in this simple model. The main result obtained for plasmons at a flat metal-dielectric interface is a relation between the lateral momentum $k_{||}$ and the frequency ω, the dispersion relation

$$k_{||}^2 = k_{photon}^2 \frac{\varepsilon_m \varepsilon_d}{\varepsilon_m + \varepsilon_d} \tag{6.1.1}$$

with the dielectric functions of metal ε_m and dielectric ε_d. $k_{photon} = \omega/c$. The derivation of Eq. (6.1.1) can be found in reference [46]. Because the surface plasmon dispersion is below the photon dispersion for all energies, it is clear that surface plasmons cannot be be excited by plane waves incident on the interface from the dielectric medium because regardless of the angle of incidence, the surface plasmon modes of the same frequency have a larger momentum. In order to excite surface plasmons, additional momentum has to be somehow provided. In practice, this is usually done either by placing a regular grating structure at the interface (which also

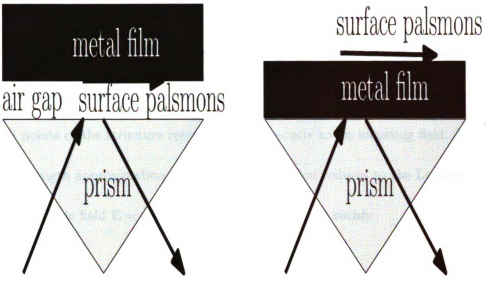

Figure 6.1: Excitation of surface plasmons. Left: Otto configuration. Right: Kretschmann configuration.

disturbs the plasmon mode) or by letting the excitation light pass through a medium with a high refractive index (e.g. a prism). In the latter case, the excitation light can either come from the side of the dielectricum (so-called Otto-configuration, Otto (1968)) or from the metal side (Kretschmann configuration, Kretschmann (1972)), cf. Fig. 6.1. In the Otto configuration, there has to be a small gap between the dielectric and the metal surface, because otherwise the surface plasmon dispersion would also be altered. In the Kretschmann configuration the metal film has to be very thin in order to allow the light field to reach through the film. The distinct resonance condition associated with excitation of surface plasmons has found applications in various sensors ranging from biological binding arrays to environmental sensing. For reviews see e.g. [27, 37].

For surface plasmons discussed above propagating on plane interface we observed that the electromagnetic field is strongly localized in one dimension, i.e., normal to

the interface. In the context of nano-optics, we are also interested in establishing field confinement in two or even three dimensions. Because the characteristic scale of the structure is much smaller than the wavelength of light, it is valid to assume that all points of the structure respond simultaneously to an incoming field. In the long wavelength approximation the Helmholtz equation reduces to the Laplace equation. The electric field $\mathbf{E} = -\nabla\Phi$ and the potential has to satisfy

$$\nabla^2\Phi = 0 \tag{6.1.2}$$

along with the boundary conditions. Let us consider a metallic nanowire with radius a centered at the origin and extending along the z-axis to infinity. The wire is exposed to an x-polarized plane radiation as depicted in Fig. 6.2. The solution of (6.1.2) turns out to be

$$\begin{aligned}
\mathbf{E_1} &= E_0\frac{2\varepsilon_d}{\varepsilon_m+\varepsilon_d}\mathbf{n}_x\ , \\
\mathbf{E_2} &= E_0\mathbf{n}_x + E_0\frac{\varepsilon_m-\varepsilon_d}{\varepsilon_m+\varepsilon_d}\frac{a^2}{\rho^2}(1-2\sin^2\varphi)\mathbf{n}_x \\
&\quad +2E_0\frac{\varepsilon_m-\varepsilon_d}{\varepsilon_m+\varepsilon_d}\frac{a^2}{\rho^2}\sin\varphi\cos\varphi\mathbf{n}_y\ .
\end{aligned}$$

From the solutions the fields diverge when $Re(\varepsilon_m) = -\varepsilon_d$, which is the resonance condition for a collective electron oscillation in a wire that is excited by an electric field polarized perpendicular to the wire axis. Notice that no resonances exist if the electric field is polarized along wire axis. The field distribution is computed for a thin

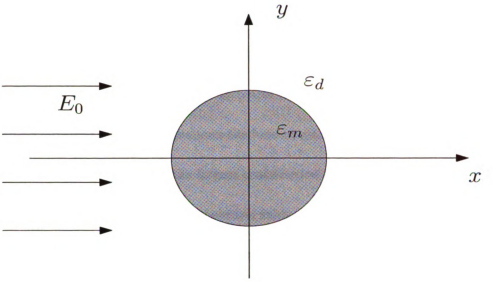

Figure 6.2: Cut through a thin wire that is illuminated by an x-polarized plane wave.

silver wire with radius 25 nm and it can be seen that the field is distributed around the wire from the second plot in Fig. 6.2. Similarly a 3D nanoparticle also support the plasmons, the solution of Eq. (6.1.2) can be obtained

$$\begin{aligned}\mathbf{E_1} &= E_0 \frac{3\varepsilon_d}{\varepsilon_m + 2\varepsilon_d}\mathbf{n}_x \\ \mathbf{E_2} &= E_0(\cos\theta\mathbf{n}_r - \sin\theta\mathbf{n}_\theta) + \frac{\varepsilon_m - \varepsilon_d}{\varepsilon_m + 2\varepsilon_d}\frac{a^3}{\rho^3}E_0(2\cos\theta\mathbf{n}_r + \sin\theta\mathbf{n}_\theta)\,.\end{aligned}$$

A strongly localized field will be obtained as $Re(\varepsilon_m) = -2\varepsilon_d$.

The near-fields around metallic nanostructures could be greatly enhanced due to the plasmons. This novel feature has enabled metallic nanostructures widely used in near-field optics, optical imaging and solar cell technology. Recently the study of surface enhanced Raman scattering (SERS) in molecule detection due to plasmons has been attracted a great deal of scientists. It was reported in 1974 that the Raman

scattering cross-section can be considerable increased if the molecules are adsorbed on rough metal surface [20], which initiated extensive researches on SERS, see e.g. [34, 43, 45, 48]. Despite all the activities in clarifying the underlying physics of SERS current theories of explaining the fundamental origin of the effect are far from satisfactory. It is accepted the largest contribution to the great signal enhancement stems from the enhanced localized electric fields in the vicinity of rough metal surfaces, a rigorous and clear physical model is still missing. Hence mathematical modeling and investigation of SERS could be a promising future direction.

6.2 Quantum dots and ultra-efficient solar cells

A solar cell or photovoltaic cell is a device that converts sunlight into electricity by photovoltaic effect. The efficiency of solar cells is the electrical power it puts out as percentage of the power in incident sunlight. One is the most fundamental limitations on the efficiency of a solar cell is the 'band gap' of the semiconducting material used on conventional solar cells: the energy required to boost an electron from the bound valence band into the mobile conduction band. When an electron is knocked loose from the valence band, it goes into the conduction band as a negative charge, leaving behind a hole of positive charge. Both electron and hole can migrate through the material. The maximum single band gap solar cell conversion efficiency is calculated to be 31 percent, termed the Shockley-Queisser limit [56]. In practice, the best achievable is about 25 percent. Stacking semiconductors with different band gaps to-

gether is one possible way to improve the efficiency. Theoretically the efficiency can be increased to higher than 70 percent by stacking dozens of different layers together in multi-junction cells. However, the crystal layers may suffer strain damages if too many layers are stacked. The most efficient multi-junction solar cell is one that has three layers: GaInP/GaAs/Ge made by the national center for photovoltaics in the US, which achieved an efficiency of 34 percent in 2001. Recent studies have shown that quantum dots offer a new possibility for improving the efficiency of solar cells. In contrast to their bulks, quantum dots possess tunable bandgap due to the quantum confinement effects. A mixture of quantum dots of different sizes used in solar cell could help harvest the maximum portion of the incident sunlight. Another advantage of quantum dots is that they can be molded into a variety of different form, in sheets or 3D arrays. A strong electronic coupling can occur between Qds if they are very close, and photongenerated excitons will have longer life, facilitating the collection and transport of electrons to produce electricity at high voltage. In addition, quantum dots array provides a possibility of multiple exciton generation (MEG) or carrier multiplication from one single photon. Researchers led by Arthur Nozik at the National Renewable Energy Laboratory Golden, Colorado in the United Sates demonstrated that the absorption of a single photon by their quantum dots yielded–not one exciton as usual the case–but three of them [17]. Also very efficient MEG was observed recently in PbSe nanocrystals by Schaller and Klimov [55]. The formation of multiple excitons per absorbed photon happens when the energy of the photon

absorbed is far greater than the semiconductor bandgap. This phenomenon does not readily occur in bulk semiconductors where the excess energy simply dissipates away as heat (interaction with phonon) before it can cause other electron-hole pairs to form. But in semiconducting quantum dots, the rate of energy dissipation is significantly reduced, and the charge carriers are confined within a minute volume, thereby increasing their interactions and enhancing the probability for multiple excitons to form. The microscopic origin of MEG is still under debate and several possibilities have been suggested in [61]: (1) Impact ionization; (2) Coherent superposition of single and multiexciton states; (3) Multiexciton formation through a virtual state. Clearly it requires more theoretical researches to clarify the underlying mechanism of MEG. To achieve a clearer picture quantum electrodynamics has to be invoked. On the other hand, optimization of structural parameters is a very important part of practical solar cell design and much more work could be done in this direction [52].

One of the ways for enhancing the conversion efficiency (increased photovoltage or increased photocurrent) can be accessed, in principle, QD solar cell configuration shown in Fig 6.3. As an attempt to a compute the its efficiency Maxwell-Garnett mixing formula (see [41] for details) is combined with the dielectric constant (3.2.7) to yield an effective dielectric constant for the colloidal quantum dot film

$$\varepsilon_{\text{eff}} = \varepsilon_{\text{e}} + 3f\varepsilon_{\text{e}}\frac{\varepsilon_{\text{i}} - \varepsilon_{\text{e}}}{\varepsilon_{\text{i}} + 2\varepsilon_{\text{e}} - f(\varepsilon_{\text{i}} - \varepsilon_{\text{e}})} \tag{6.2.1}$$

This mixing rule predicts the effective dielectric ε_{eff} of a heterogeneous medium

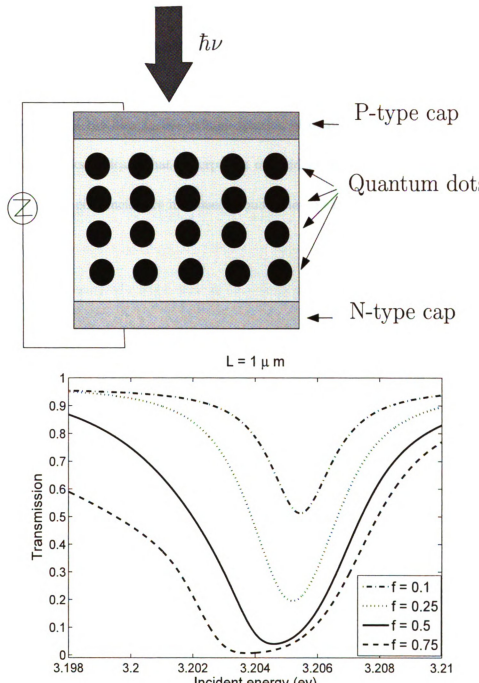

Figure 6.3: Top: A colloidal QD array used as a photoelectrode for a photochemical or as the i-region of a p-i-n solar cell; Bottom: The transmission as a function of incident energy and volume fraction of QD. The peaks indicate absorbtion enhancements.

where homogeneous quantum dots with ε_i are dilutely mixed into istropic environment ε_e. The inclusions occupy a volume fraction f. It should be noted that the formula above assumes a uniformly distribution and well separations of quantum dots. The numerical results show that resonant peaks depend on several parameters, the thickness of the film L, the volume fraction of quantum dots, the incident energy. Those peaks indicate that absorptions of incident light achieve maxima and hence conversion efficiencies are increased around these peaks.

Bibliography

[1] I. Abram, *Nonlinear-optical properties of biexcitons: Single-beam propagation*, Phys. Rev. B, 28 (1983) pp. 4433–4443.

[2] I. Abram and A. Maruani, *Calculation of the nonlinear dielectric function in semiconductors*, Phys. Rev. B, 26 (1982) pp. 4759–4761.

[3] I. Abram, A. Maruani and S. Schmitt-Rink, *The non-linear susceptibility of the biexciton two-photon resonance*, J. Phys. C : Solid State Phys., 17 (1984) pp.

5163–5170.

[4] H. Ajiki and K. Cho, *Longitudinal and transverse components of excitons in a spherical quantum dot*, Phys. Rev. B, 62 (2000), pp. 7402-7412.

[5] G. Bao and Y. Sun, *Modeling and computation of the scattering by a nano optical medium*, Contemp. Math., to appear.

[6] G. Bao and Y. Sun, *Optical polariton modes in a nanoscale semiconductor*, submitted.

[7] F. Bassania, G. La Roccaa and M. Artonib, *Electromagnetic induced transparency in bulk and microcavity semiconductors*, J. Lumi., 110 (2004) pp. 174-180.

[8] M. Born and E. Wolf, *Principles of optics : electromagnetic theory of propagation, interference and diffraction of light*, Cambridge University Press, New York, 1999.

[9] P. Borri, W. Langbein, U. Woggon, A. Esser, J. Jensen and J. Hvam, *Biexcitons in semiconductor microcavities*, Semicond. Science and Technol., 18 (2003) pp. S351–S360.

[10] R.W. Boyd, *Nonlinear Optics*, Academic Press, San Diego, 2003.

[11] S. Chesi, M. Artoni, G. La Rocca, F. Bassani and A. Mysyrowicz, *Exciton-biexciton quantum coherence and polaritonic stop-band transparency in CuCl*, Phys. Stat. Sol., 1 (2004) pp. 497–500.

[12] K. Cho, *Optical Response of Nanostructures: Microscopic Nonlocal Theory*, Springer-Verlag, New York, 2003.

[13] D. Craig and T. Thirunanachandran, *Molecular Quantum Electrodynamics*, Dover Pulications, Inc, Mineola, New York, 1998.

[14] C. Cohen-Tannoudji, J. Dupond-Roc, and G. Grynberg, *Photons and Atoms*, John Wiley & Sons, New York, 1997.

[15] A. D'Andrea, R. Del Sole. *Wannier-Mott excitons in semi-infinite crystals: Wave functions and normal-incidence reflectivity*, Phys. Rev. B, 25 (1982), pp. 3714–3730.

[16] A. Ekimov, A. Efros and A. Onuschchenko, *Quantum size effect in semiconductor microcrystals*, Solid State Commun., 56 (1985) pp. 921–924.

[17] R. Ellingston, M. Beard, J. Johnson, P. Yu, O. Micic, A. Nozik, A. Shabaev and A. Efros, *Highly Efficient Multiple Exciton Generation in Colloidal PbSe and PbS Quantum Dots*, Nano Lett., 5 (2005) pp. 865–871.

[18] B. Engquist and A. Majda, *Absorbing boundary conditions for the numerical simulation of waves*, Math. Comp., 31 (1977) pp. 629–651.

[19] L. Evans, *Partial differential equations*, American Mathematical Society, Providence, Rhode Island, 1998.

[20] M. Fleischmann, P.J. Hendra and A.J. McQuillan, *Raman scattering of pyridine adsorbed at a silver electrode*, Chem. Phys. Lett., 26 (1974) pp. 163–166.

[21] J. Frenkel, *On the transmission of light into heat in solids*, Phys. Rev., 37 (1931) pp. 17–44.

[22] S. Gasiorowicz, *Quantum Physics*, Wiley, New York, 1996.

[23] G. Grosso and G. P. Parravicini, *Solid State Physics*, Academic Press, San Diego, 2003.

[24] E. Hanamura, *Very large optical nonlinearity of semiconductor microcrystallites*, Phys. Rev. B, 37 (1988), pp. 1273–1279.

[25] M. Hasuo and N. Nagasawa, *Bose-Einstein Condensation*, Cambridge University Press, Cambridge, 1995.

[26] F. Henneberger and V. May, *Nonlinear energy transport of radiation in dielectrics due to virtual biexciton formation*, Phys. Status Solidi (b), 108 (1981) pp. 377–387.

[27] J. Homola, S.S. Yee and G. Gauglitz, *Surface plasmons resonance sensors: review*, Sensors and Actuators B, 54 (1999) pp. 3–15.

[28] J. Hopfield, D. Thomas, *Theoretically and experimental effects of spatial dispersion on the optical properties of crystal*, Phys. Rev., 132 (1963), pp. 563–572.

[29] J. Jackson, *Classical Electrodynamics*, Wiley, New York, 1999.

[30] A.M. Janner, *Second harmonic generation, a selective probe for excitons*, Ph.D. Thesis, University of Groningen, Groningen, Netherlands, 1998.

[31] T. Kato, *Perturbation Theory for Linear Operators*, Springer-Verlag, Berlin, 1980.

[32] O. Keller, *Local fields in the electrodynamics of mesoscopic media*, Phys. Rep., 268 (1996), pp. 85-262.

[33] C. Klingshirn, *Semiconductor Optics*, Spring-Verlag, New York, 2007.

[34] K. Kneipp, Y. Wang, H. Kneipp, L.T. Perelman, I. Itzkan, R.R. Dasari and M.S. Feld, *Single molecule detection using surface-enhanced Raman scattering (SERS)*, Phys. Rev. Lett., 78 (1997) pp. 1667–1670.

[35] M. Lampert, *Mobile and immobile effective-mass-particle complexes in nonmetallic solids*, Phys. Rev. Lett., 1 (1958) pp. 450-453.

[36] W. Liang, *Excitons*, Phys. Educ. **5**, 226 (1970).

[37] B. Liedberg, C. Nylander and I. Lundstrom, *Surface-plason resonance for gas-detection and biosensing*, Sensors and Actuators, 4 (1983) pp. 299–304.

[38] R. Loudon, *The Quantum Theory of Light*, Oxford University Press, Oxford, 1983.

[39] R. März, S. Schmitt-Rink and H. Haug, *Optical properties of dense exciton-biexciton systems*, Z. Phys. B, 40 (1980) pp. 9–14.

[40] P. Milloni and J. Eberly, *Lasers*, John Wiley and Sons, New York, 1988.

[41] G.W. Milton, *The Theory of Composites*, Cambridge University Press, Cambridge, 2002.

[42] A. Mysyrowicz, *Bose-Eintein Condensation*, Cambridge University Press, Cambridge, 1995.

[43] S. Nie and S.R. Emory, *Probing single molecules and single nanoparticles by surface-enhanced Raman scattering*, Science, 275 (1997)

pp. 1102–1106.

[44] M. Nirmal, D. Norris, M. Kuno, em et al., *Observation of the 'dark exciton' in CdSe quantum dots*, Phys. Rev. Lett., 75 (1995) pp. 3728–3731.

[45] L. Novotny and C. Hafner, *Light propagation in a cylindrical waveguide with a complex, metallic, dielectric function*, Phys. Rev. E, 50 (1994) pp. 4094–4106.

[46] L. Novotny and B. Hecht, *Principles of Nano-Optics*, Cambridge University Press, New York, 2007.

[47] A.J. Nozik, *Spectroscopy and Hot Electron Relaxation Dynamics in Semiconductor Quantum Wells and Quantum Dots*, Annu. Rev. Phys. Chem., 52 (2001) pp. 193–231.

[48] A. Otto, I. Mrozek, H. Grabhorn and W, Akemann, *Surface-enhanced Raman scattering*, J. Phys.: Condens, Matter, 4 (1992) pp. 1143–1212.

[49] S. Pekar, *The theory of electromagnetic waves in crystal in which excitons are produced* , Sov. Phys. JETP, 6 (1958), pp. 785-796.

[50] M. Reed, Scientific American **268**, 118 (1993).

[51] R. Rossetti, L. Ellison, J. Gibson and L. Brus, *Size effects in the excited electronic states of small colloidal CdS crystallites* J. Chem. Phys., 80 (1984) pp. 4464–4469.

[52] J. Robinson and Y. Rahmat-Samii, *Particle swarm optimization in electromagnetics*, IEEE Trans. Antennas and Propagat. 52 (2004) pp.397–407.

[53] R. Rossetti, S. Nakahara and L. Brus, *Quantum size effects in the redox potentials, resonance Raman spectra, and electronic spectra of CdS crystallites in aqueous solution*, J. Chem. Phys., 79 (1983) pp. 1086–1088.

[54] J.J. Sakurai and S.F. Tuan, *Modern Quantum Mechanics*, Benjamin/Cummings, Menlo Park, 1985.

[55] R. Schaller and V. Klimov, *High Efficiency Carrier Multiplication in PbSe Nanocrstals: Implications for Solar Energy Conversion*, Phys. Rev. Lett., 92 (2004) pp. 186601-1–4.

[56] W. Shockley and H. Queiser, *Detailed Balance Limit of Efficiency of p-n Junction Solar Cells*, J. Appl. Phys., 32 (1961) pp. 510–519.

[57] L. Silverstri, G. Czajkowski and F. Bassani, *Density matrix approach to electromagnetic wave scattering of a quantum dot*, Phys. Stat. Sol. (a), 175 (1999) 383–391.

[58] A. Stahl and I. Balslev, *Electrodynamics of the Semiconductor Band Edge*, Springer Tract in Mod. Phys. 110, Springer-Verlag, New York, 1987.

[59] Y. Sun, H. Ajiki and G. Bao, *Computational modeling of optical response from excitons in a nano optical medium*, Comm. Comput. Phys., 4 (2008) pp. 1051–1068.

[60] Z.K. Tang, A. Yanase, T. Yasui, Y. Segawa, and K. Cho, *Optical selection rule and oscillator strength of confined exciton system in CuCl thin films*, Phys. Rev. Lett., 71 (1993), pp. 1431-1434.

[61] D. Timmerman, I. Izeddin, P. Stallinga, I. N. Yassievich and T. Gregorkiewicz, *Space-separated quantum cutting with silicon nanocrystals for photovoltaic applications*, Nature Photonics, 2 (2008) pp. 105–109.

[62] H. C. Van De Hulst, *Light Scattering by Small Particles*, John Willey & Sons, New York, 1957.

[63] M. Verweij, *Four ways of deducing Maxwell's equations from their microscopic counterparts - Lorentz's theory of electrons revisited*, Proceedings of the 27th General Assembly of the International Union of Radio Science, Maastricht, The Netherlands, 17-24 August 2002.

[64] J. Warnock and D. Awschalom, *Quantum size effects in simple colored glass*, Phys. Rev. B, 32 (1985) pp. 5529–5531.

[65] J. Zheng, C. Zhang, and R.M. Dickson, *Highly fluorescent, water-soluable, size-tunable gold quantum dots*, Phys. Rev. Lett., 93 (2004) pp. 077402-1–4.

[66] P. Zory, Jr, *Quantum Well Lasers* (Academic Press, 1993).